A MULTIPHASE ANALYSIS FOR ENVIRONMENTAL IMPACT ASSESSMENT WITH θ -STOCK FINITE ELEMENT PROGRAM

B. GATMIRI
University of Tehran, Tehran, Iran
Université Paris-Est, Laboratoire Navier (ENPC/LCPC/CNRS)
Ecole des Ponts ParisTech, 6 and 8 av Blaise Pascal
77455 Marne-la-Vall´ee, France
Actually National Radioactive Waste Management Agency, France
behrouz.gatmiri@andra.fr

S. HEMMATI
Université Paris-Est, Laboratoire Navier (ENPC/LCPC/CNRS)
Ecole des Ponts ParisTech
Actually Ecole Centrale Paris, France
sahar.hemmati@ecp.fr

C. ARSON
Université Paris-Est, Laboratoire Navier (ENPC/LCPC/CNRS)
Ecole des Ponts ParisTech
Actually Texas A&M University, USA
carson@civil.tamu.edu

E. AMIRZEHNI
Civil Engineering Department
University of Tehran, Tehran, Iran

In the THM modeling of multiphase medium, the coupling effects of skeleton, suction, and temperature have been integrated via the concept of state surfaces of void ratio and degree of saturation. Based on proposed formulation, a fully coupled numerical model for the behavior of soil deformation, water flow, air flow, heat flow in unsaturated soil has been developed and integrated in a finite element code θ-Stock by the first author. This program is conceived with this idea that it will be able to analyze the response of a soil in different states of humidity to mechanical, thermal loading, and also damage phenomena. Damage model is dedicated to unsaturated brittle rocks. It mixes phenomenological and micromechanical concepts and is formulated based on the use of independent state variables. The expression of the liquid permeability is modified in order to represent the influence of fracturing on interstitial fluid flows. The final matrix form of established field equations of the proposed model for unsaturated case

has been encoded for this particular purpose, in a finite element program which had been developed for dry and saturated soils previously.

Keywords: Multiphase porous media; finite elements method; damage; thermo-hydromechanics; root water uptake; pollutant transport; soil–atmosphere interaction.

1. Introduction

In compacted fills or in arid climate areas where soils are submitted to wetting–drying cycles, fine-grained soils are not saturated with water, and contain some air. Due to capillary effects and soil–clay adsorption, the pore water is no more positive and is subjected to suction. It has been shown that a multiphysical approach should be used in different scales from nano to macro in order to model the behavior of soil skeleton in clayey soil or clay rocks. The problem becomes more difficult when considering the coupling effects in multiscale and multiphase modeling. In unsaturated soils, various researchers demonstrated that the effective stress concept was not satisfactory to describe the volume change behavior of unsaturated soil. The main problem is observed when an unswelling unsaturated soil is loaded and soaked. The soil shows a volume decrease (collapse), whereas effective stress analyses predict a swelling.

A fully thermohydromechanical (THM) coupled model for saturated soils has been implemented in the finite element software θ-Stock by the first author. The formulation of effective stresses is based on an extension of the Biot's theory. The elastoplastic Cam–Clay model has been modified to include suction and temperature effects, by introducing state surfaces for the void ratio and the saturation degree.[1–4]

Various constitutive laws have been used in THM model, such as the incremental elastic formulation suggested by Coleman and Fredlund. Matyas and Radhakrishna proposed a state surface concept in order to describe the changes of volume and degree of saturation as a function of mean net stress and suction. Lloret and Alonso and Gatmiri and Delage proposed mathematical expressions for these surfaces, in the framework of nonlinear elastic behavior. The elastic and nonlinear stress strain behavior was based on a Kondner–Duncan hyperbolic model.

The θ-Stock code described in this paper is derived from this approach, with some modifications. The numerical resolution is fully coupled and a different expression of the state surface is adopted in order to ensure compatibility between the state surface and the hyperbolic stress–strain model. Relevant equations, numerical algorithms, and two graphic tools for pre- and post-processing for the finite element models are described. Their main options are summarized as well.

Also, the θ-Stock code deals with the modeling of the behavior of the massif neighboring a nuclear waste repository before waste disposal. Risks of radionuclide percolation have to be assessed in order to ensure the safety of nuclear waste repositories. It is thus necessary to characterize the EDZ (excavation damaged zone) surrounding storage galleries.[5–8]

During the excavation phase, the soil can be damaged by tensile fractures. Pore water is drained toward the drift. Drainage may be accelerated by the growth of permeability induced by the existence of a connected crack network. Once the support has been built, water remains trapped behind concrete. Around the gallery, the soil is generally almost saturated. Suction in the soil mass tends to reverse the orientation of the water flow. The back pressure exerted by the support induces compressive stresses which tend to close the fractures. The presence of water can trigger the precipitation of minerals contained in the host plastic clay, generating a chemical healing. When waste is disposed in the tunnel, heat solicitations induce an increase of suction, and the resulting tensile stresses may fracture again the geological barrier. As the temperature decreases, drying effects weaken, leading to a possible resaturation. The suction increase is equivalent to a compressive loading, since it diminishes tensile stresses. A second mechanical healing process may be considered.

Physically, the damage concept must represent the degradation of elastic properties and the increase of permeability due to the growth of connected porosity. Mathematically, the formulation has to be compatible with the existing developments implemented in θ-Stock.

In this paper, a two-dimensional model for soil–atmosphere interaction developed by considering the mass and energy balance equations is presented. This model is integrated in θ-Stock. The exchange of moisture and heat between a multiphase soil and an atmosphere layer is simulated. Considering the latent and sensible heat transport equations and consequently the moisture exchange (evaporation and condensation), equations are developed by taking into account climatic measured factors such as wind, temperature, precipitation, humidity, and radiation. The model of boundary conditions is coupled with a system of equations incorporating THM behavior for multiphase medium integrated in θ-Stock.

On the other hand a set of equations was presented to calculate the rate of root water uptake in each point of unsaturated soil. Geotechnical engineers usually do not pay attention to the change of moisture content and groundwater level of the projects and assume that the soil condition will always remain unchanged after the time of study. Indeed, soil–atmosphere interaction can severely change the moisture content of the soil. For instance, heavy rainfall, evapotranspiration, and change in groundwater table can have significant effects on the moisture condition in the soil. Among the above-mentioned parameters, transpiration from vegetation's leaf surface is of most significance. This model has been integrated in finite element code of θ-Stock in order to carry out a fully coupled simulation of the effect of vegetation water uptake in unsaturated porous media.

After a brief description of thermohydromechanical behavior of unsaturated media, the extension of THM models to thermohydrochemomechanical (THCM) models is discussed for the general conditions. Pollutant transport in soil has become a major issue of concern in recent years. The problems in the environmental geomechanics often involve the study of heat, mass, and contaminant transport

in a number of engineering situations. Increased awareness of the damage caused by industrial activities, coupled with the need of development of a sustainable industrial society have highlighted the importance of this subject. The pollutant transport normally takes place in the unsaturated soil and in the presence of heat changes due to climate changes or radionuclear waste disposal. This paper gives the governing equations of the thermohydrochemomechanical behavior in order to evaluate the change of chemical concentration in a multiphase medium.

Theoretical and numerical developments for this complex formulation are presented and the integration of it in θ-Stock software is described.

2. Unsaturated Porous Media Under Heating

The model presented in this paper is a model in which two basic theories have been modified and combined in order to describe a fully coupled behavior of unsaturated porous medium under heating. On one hand the nonlinear theory of isothermal behavior of unsaturated soil under coupled effects of net stress and suction via the concept of state surface of void ratio and degree of saturation based on previous works of the first author[2,9,10] is modified and extended to nonisothermal behavior. On the other hand the Philip and de Vries' theory of heat and moisture transfer is modified in order to consider the deformation of skeleton and to be presented in a new form, suction-based formulation, which is more suitable for combination with deformation theory of unsaturated soils. The basic assumptions considered in this development are the following:

- The medium consists of superposition of three continuous media.
- The poroelastic medium constituting the skeleton is isotropic and nonlinear.
- Quasi-static conditions and small transformation are considered.
- Fluids and solid grains are compressible.
- Energy transfer by all phases, and phase changes between liquid and gas are considered.
- Generalized Darcy's law is valid for motion of water and dry air.
- Fourier's law is considered for conductive heat flow.
- Solid and pore water densities are pressure- and temperature-dependent.
- Air and water permeabilities depend on matrix suction, strain level, and temperature.
- Void ratio and degree of saturation state surfaces are temperature-dependent.
- Thermal expansion coefficient of mixture depends on suction, stress, and temperature.
- Dissolving of air in water is considered.
- Vapor pressure and thermal gradient are considered.
- The state variables are the net total stress $\sigma - P_a$, matrix suction $P_a - P_w$, and temperature T which leads, in numerical formulation, to five degrees of freedom.
- Creep phenomenon is neglected.

2.1. *Theoretical formulation*

2.1.1. *Moisture phase movement equation*

The moisture has been consisted of vapor and liquid. The term *liquid transfer* will be used for the transfer which occurs exclusively in liquid phase, and all transfer in excess of the liquid transfer is named *vapor transfer* as they are used by Philip and de Vries.[11]

2.1.1.1. Vapor transfer

The equation of vapor diffusion in porous media according to Krischer and Rohnalter[12] and Philip and de Vries[11] can be given as follows:

$$q_{\text{vap}} = -D_0 \cdot \nu \cdot \alpha \cdot a \cdot \nabla \rho_v \tag{1}$$

in which q_{vap} is the vector of vapor flux density, $\text{kg} \cdot \text{m/m}^2\text{s}$; D_0 is the molecular diffusivity of water vapor in air, m^2s; ν is the *mass flow factor* introduced to allow for the mass flow of vapor arising from the difference in boundary conditions governing the air and vapor components of the diffusion system; it is given by the expression: $\nu = P_g/(P_g - P_v)$ where P_v is partial pressure of vapor. Also, α is a tortuosity factor; a is volumetric air content which can be expressed by $a = n(1 - S_r)$ with n the porosity and S_r degree of water saturation; ρ_v is the density of water vapor, $\text{kg} \cdot \text{m/m}^3$.

Krischer and Rohnalter[12] have given an expression for evaluation of D_0:

$$D_0 = \frac{244 \times 10^{-7}}{P_g} \left(\frac{T}{273} \right)^{2.3}, \tag{2}$$

with P_g in bars, and this equation gives D_0 in m/s. The dependence of the coefficient of diffusion of vapor on the porosity of a soil is investigated experimentally by Penman.[13]

For a limited range of values of $n (0.0 < n < 0.7)$ he has proposed to reduce this coefficient by a factor of $0.66n$. The tortuosity effect is incorporated in this factor.

To find ρ_v, the following thermodynamic relationships can be introduced:

$$\rho_v = \rho_0 \cdot h\,, \tag{3}$$

$$h = \exp\left[\frac{\psi \cdot g}{R \cdot T} \right], \tag{4}$$

where ρ_0 is the density of saturated water vapor, kgm/m^3; h is relative humidity; R is the gas constant $(R = 4.615 \times 10^6)$; and ψ is thermodynamic potential of water in soil.

Another relationship for relative humidity is proposed by Geraminegad and Saxena[14]:

$$h = \left[1 + \left(\frac{\theta}{0.04\rho_0} \right)^{-4.27} \right]^{-0.42}. \tag{5}$$

Based on Philip and de Vries,[11] in further development, it is supposed that $\partial h/\partial T = 0$, and for density of saturated vapor ρ_0, the following relationship which is given by Geraminegad and Saxena[14] is used:

$$\frac{1}{\rho_0} = 194.4 \exp(-0.06374T + 0.1634 \times 10^{-3} T^2)\,. \tag{6}$$

The final θ-based formulation of vapor velocity equation can be given as follows:

$$V = \frac{q_{\text{vap}}}{\rho_w} = -D_{Tv}\nabla T - D_{\theta v}\nabla\theta\,, \tag{7}$$

where D_{Tv} is thermal vapor diffusivity and $D_{\theta v}$ is isothermal vapor diffusivity which are given as follows:

$$D_{Tv} = \frac{D_0}{\rho_w}\cdot\nu\cdot n\cdot h\frac{(\nabla T)_a}{\nabla T}\cdot\frac{d\rho_0}{dT} \quad \theta < n\,, \tag{8}$$

$$D_{\theta v} = \frac{D_0}{\rho_w}\cdot\nu\cdot n\cdot\frac{\rho_0 hg}{RT}\frac{\partial\psi}{\partial\theta} \quad \theta < n \tag{9}$$

in which

$$\frac{(\nabla T)_a}{\nabla T} = \frac{1}{3}\left[\frac{2}{1+BG} + \frac{1}{1+B(1-2G)}\right], \tag{10}$$

$$B = \frac{\lambda a + \lambda v}{\lambda w} - 1\,, \tag{11}$$

$$G = \begin{cases} 0.3333 - 0.325\,\dfrac{n-\theta}{n} & 0.09 < \theta < n\,, \\ 0.0033 + 11.11\,\theta\left(0.33 - 0.325\,\dfrac{n-0.09}{n}\right) & 0 < \theta < 0.09\,, \end{cases} \tag{12}$$

$$\begin{aligned} \lambda_a &= 0.0258\,\text{w/mK}\,, \\ \lambda_v &= D_0\cdot\nu\cdot h\cdot h_{fg}\cdot\frac{d\rho_0}{dT}\,, \\ \lambda_w &= 0.6\,\text{w/mK}\,, \end{aligned} \tag{13}$$

where h_{fg} is latent heat of vaporization of soil water,
λ_v is vapor thermal conductivity,
λ_a is air thermal conductivity,
λ_w is water thermal conductivity.

This form will be converted to suction-based formulation.

2.1.1.2. Liquid phase transfer

A generalized Darcy's law for unsaturated soil can be considered as follows:

$$U = \frac{q_w}{\rho_w} = -K\nabla(\psi + z)\,, \tag{14}$$

U is liquid velocity, q_w is vector of fluid flow, ρ_w is density of fluid, K is permeability, ψ is capillary potential, and z is elevation (gravitational potential).

The final θ-based form of fluid motion in unsaturated porous media:

$$U = \frac{q_w}{\rho_w} = -D_{Tw}\nabla T - D_{\theta w}\nabla\theta - D_w\nabla Z\,, \tag{15}$$

where D_{Tw} is thermal liquid diffusivity,

$$D_{Tw} = K(\theta, T)\,\frac{\psi_r(\theta)}{\sigma_r}\frac{d\sigma(T)}{dT}\,, \tag{16}$$

$D_{\theta W}$ is isothermal liquid diffusivity,

$$D_{\theta w} = K(\theta, T)\frac{\sigma(T)}{\sigma_r}\frac{d\psi_r}{d\theta}\,, \tag{17}$$

D_W is gravitational diffusivity,

$$D_w = K(\theta, T)\,. \tag{18}$$

2.1.1.3. Total moisture transfer

The total moisture movement in unsaturated soil due to temperature gradient and its resulting moisture content gradient is equal to the sum of the flows which take place in phases, vapor and liquid. Thus,

$$\frac{q}{\rho_w} = -D_T\nabla T - D_\theta\nabla\theta - D_w\nabla Z\,, \tag{19}$$

where D_T is thermal moisture diffusivity and is equal to $D_{Tv} + D_{Tw}$, D_θ is isothermal moisture diffusivity, and is equal to $D_{\theta v} + D_{\theta w}$.

2.1.2. *Moisture mass conservation*

A suction-based formulation of moisture movement equation can be found:

$$\begin{aligned} &nS_r\beta_T\frac{\partial T}{\partial t} + nS_r\beta_P\frac{\partial p_w}{\partial t} + (\rho_w - \rho_v)n\frac{\partial S_r}{\partial t} \\ &\quad + (S_r\rho_w + \rho_v(1 - S_r))\frac{\partial n}{\partial t} + n\,(1 - S_r)\frac{\partial \rho_v}{\partial t} \\ &\quad = \operatorname{div}(\rho_w D_w\nabla z) + \operatorname{div}(\rho_w D_\theta\nabla T) + \operatorname{div}(\rho_w D_p\nabla(P_w - P_g)) + Q_m \end{aligned} \tag{20}$$

with

$$D_{Pw} = K(\theta, T)\frac{\sigma(T)}{\sigma_r\cdot\gamma_w}\,, \tag{21}$$

$$D_{Pv} = \frac{D_0}{\rho_w}\nu\cdot n\frac{\rho_v g}{RT\cdot\gamma_w}\cdot\frac{\sigma(T)}{\sigma_r}\,, \tag{22}$$

$$D_P = D_{Pw} + D_{Pv}, \tag{23}$$

$$D_P = K(\theta, T)\frac{\sigma(T)}{\sigma_r\cdot\gamma_w} + \frac{D_0}{\rho_w}\nu\cdot n\frac{\rho_v g}{RT\cdot\gamma_w}\cdot\frac{\sigma(T)}{\sigma_r}\,, \tag{24}$$

in which surface energy can be written as

$$\sigma(T) = -75.882 + 0.165T\,, \tag{25}$$

where T is temperature in degree Celsius and σ is surface energy in dyne/cm^2.

2.1.3. *Gas flow equation*

Considering the Darcy's law and P_g as a function of temperature ($P_g = P_g(T)$), the gas flow equation can be given as

$$V_g = \frac{-K_g}{\gamma_g}\frac{\partial P_g}{\partial T}\nabla T - K_g\left(\nabla\left(\frac{P_g}{\gamma_g}\right) + \nabla Z\right), \tag{26}$$

where V_g is vector of gas velocity, q_g is vector of gas flow, ρ_g is density of gas, K_g is air permeability, P_g is gas pressure, γ_g is specific weight of gas, ∇Z is elevation, and

$$K_g = \frac{b\gamma_g}{\mu_g}[e(1 - S_r)]^c\,, \tag{27}$$

where b and c are the constants. In Eq. (27), gas permeability is assumed to be a function of water content and it does not depend on temperature.

2.1.4. *Mass conservation of air*

The governing differential equation of mass conservation of air in a control volume of an unsaturated porous media can be given as

$$\frac{\partial}{\partial t}[n\rho_g(1 - S_r + HS_r)] = -\mathrm{div}(\rho_g V_g) - \mathrm{div}(\rho_g HU) + \rho_w \,\mathrm{div}\, V\,, \tag{28}$$

where H is Henry constant which is equal to 0.02.

The first term of the right-hand side is related to gas flow due to gas pressure gradient and the second term denotes the motion of dissolved gas in the liquid while the gas loss by vapor condensation is presented by the third term.

2.1.5. *Heat flow*

Total flow of latent and sensible heat in an unsaturated porous medium is given based on Philip and de Vries theory as

$$\begin{aligned} Q = {} & -\lambda \,\mathrm{grad}\, T + [C_{Tw}\rho_w U + C_{Tv}\rho_w V + C_{Tg}\rho_g V_g]\,(T - T_0) \\ & + \rho_w h_{fg} V + \rho_v V_g h_{fg}\,, \end{aligned} \tag{29}$$

where λ accounts for Fourier heat diffusion coefficient and can be evaluated by following proposition:

$$\lambda = (1 - n)\lambda_s + \theta\lambda_w + (n - \theta)\lambda_v\,. \tag{30}$$

Through this equation which gives the upper limit of heat conductivity in unsaturated porous media, the continuity between saturated and unsaturated case is

ensured. In this equation, ρ_s is density of solid grain, ρ_w is density of liquid, ρ_v is density of vapor, ρ_g is density of gas, C_{Ts} is specific heat capacity of solid, C_{Tw} is specific heat capacity of liquid, C_{Tv} is specific heat capacity of vapor, C_{Tg} is specific heat capacity of gas, T_0 is an arbitrary reference temperature, and h_{fg} is latent heat of vaporization.

In Eq. (29), the first term denotes the conductive heat flow, the second term is related to the convective heat flow in liquid, vapor, and gas, and the two last terms denote the latent heat related to evaporation.

2.1.6. *Energy conservation equation*

Energy conservation equation in a porous medium can be expressed by

$$\frac{\partial \varphi}{\partial t} + \operatorname{div} Q = 0\,, \tag{31}$$

in which Q is heat flow and φ is the volumetric bulk heat content of medium which can be defined by

$$\varphi = C_T(T - T_0) + (n - \theta)\rho_v h_{fg}\,, \tag{32}$$

where C_T is the specific heat capacity of unsaturated mixture and can be written as

$$C_T = (1 - n)\rho_s C_{Ts} + \theta\rho_w C_{Tw} + (n - \theta)\rho_v C_{tv} + (n - \theta)\rho_g C_{Tg}\,. \tag{33}$$

2.1.7. *Solid skeleton*

Strain increment due to total net stress changes in unsaturated soil is generally presented by an expression such as

$$d\varepsilon = D^{-1} d(\sigma - mP_g)\,, \tag{34}$$

where D is an elastic stress–strain relationship matrix.

By combining the strain increments due to suction changes $d(P_g - P_w)$ and temperature increment dT, the constitutive law of solid skeleton in unsaturated porous medium can be presented by

$$d(\sigma_{ij} - \delta_{ij} p_g) = Dd\varepsilon - Fd(p_g - p_w) - CdT\,, \tag{35}$$

where

$$\begin{aligned}
&F = DD_s^{-1} \quad \text{with} \quad D_s^{-1} = \beta_s m, \text{ in which}\\
&\beta_s = \frac{1}{1+e}\frac{\partial e}{\partial (p_g - p_w)} \quad \text{and} \quad m^T = [1 \quad 1 \quad 0]\,,\\
&C = DD_T^{-1} \quad \text{with} \quad D_T^{-1} = \beta_t m\,, \text{ in which}\\
&\beta_t = \frac{1}{1+e}\frac{\partial e}{\partial T}\,.
\end{aligned} \tag{36}$$

Assuming nonlinear elastic behavior, using Kondner–Duncan (hyperbolic) model isothermal tangent elastic modulus with a hyperbolic variation can be given:

For loading:

$$E_L = K_L P_{\text{atm}} \left(\frac{\sigma_3}{P_{\text{atm}}} \right)^n (1 - R_f S_r)^2 \,. \tag{37}$$

For unloading:

$$E_u = K_u P_{\text{atm}} \left(\frac{\sigma_3}{P_{\text{atm}}} \right)^n \,, \tag{38}$$

with $S_r = (\sigma_1 - \sigma_3)/(\sigma_1 - \sigma_3)_{\text{ult}}$ stress ratio, σ_1 and σ_3 principal stresses, P_{atm} is atmosphere pressure, K_L and K_u are modulus numbers (dimensionless), n and R_f are constants.

Considering the effect of the heating, the above equations become

Loading:

$$E = (E_i + E_t)\,(1 - R_f S_r)^2 \,. \tag{39}$$

Unloading:

$$E = E_i + E_t \,, \tag{40}$$

with

$$E_L = K_L P_{\text{atm}} \left(\frac{\sigma_3}{P_{\text{atm}}} \right)^n \,, \tag{41}$$

$$E_t = m_1 \cdot T \,. \tag{42}$$

To calculate the bulk modulus, the volumetric strain can be taken into account via void ratio state surface which depends on stress, suction, and temperature. Using the same approach for determination of state surface of void ratio which is used by Gatmiri,[1,3] and Gatmiri and Delage,[36] a new formulation of void ratio state surface is proposed as follows:

$$\begin{aligned} e &= \frac{1 + e_0}{\exp\left[\dfrac{A}{K_b(1-m)}\right] \exp[c_e(T - T_0)]} - 1 \,, \\ A &= \left[a \left(\frac{\sigma - p_g}{p_{\text{atm}}} \right) + b \left(1 - \frac{\sigma - p_g}{\sigma_c} \right) \left(\frac{p_g - p_w}{p_{\text{atm}}} \right) \right]^{1-m} \,, \end{aligned} \tag{43}$$

where a_e, b_e, and c_e are constants, and σ_e is the preconsolidation stress. Through this equation the compatibility with nonlinear behavior of soil is ensured.

Besides stress–strain behavior coupled with temperature, the description of coupled state of volumetric moisture content with temperature of unsaturated soil is also necessary under the stress and suction effects. On the basis of experimental data the following state surface of degree of saturation is proposed:

$$S_r = 1 - [a_s + b_s(\sigma - p_g)] \times [1 - \exp(c_s(p_g - p_w))] \exp(d_s(T - T_0)) \,, \tag{44}$$

in which a_s, b_s, c_s, d_s are constants.

To evaluate the elastic tangent modulus E given by Eq. (39), the shear strength should be defined considering the influence of suction and temperature on the cohesion and friction angle. The lack of reliable information about the effect of temperature on the shear strength of the soils leads, for instance, to consider an approximate evaluation of shear strength variation under heating based on the suggested formula for the friction angle variation under the temperature change given by Houston *et al.*[15] such as

$$\varphi_{(T)} = \varphi_0 \exp(0.002\,T)\,. \tag{45}$$

Based on experimental results of CERMES, the following equations can be proposed for the effect of suction:

$$\tau_{\text{rup}} = C_{(s)} + \sigma_n tg\varphi_{(s)}\,, \tag{46}$$

with

$$C_{(s)} = C' + m_2(P_g - P_w)\,, \tag{47}$$

$$\varphi_{(s)} = \varphi_{\text{ult}} + (\varphi_{\text{in}} - \varphi_{\text{ult}})\left(1 - \frac{(P_g - P_w)}{(P_g - P_w)_{\text{ult}}}\right), \tag{48}$$

where m_2 is a constant, φ_{in} is the initial friction angle, and φ_{ult} is the friction angle under final suction. The parameters of this model are described in detail by Gatmiri *et al.*[16,51]

2.2. *Material properties*

2.2.1. *Heat transfer parameters*

Since the soil components consist of solid skeleton, air and water, the thermal behavior of soil is affected by their respective properties and the influence of temperature.

The most important thermal properties are thermal conductivity of soil.

With the assumption of parallel flow in solid and moisture phases, one can find

$$\lambda = (1-n)\lambda_s + \theta\lambda_w + (n-\theta)\lambda_v\,. \tag{49}$$

This equation is used in this study, and implicitly the continuity of moisture is assumed.

The other thermal parameters considered in the development of the model are C_{Ps}, C_{Pw}, C_{Pv}, and C_{Pg}, the specific heat capacity of solid, water, vapor, and gas, respectively, which are involved in the following term:

$$C_T = (1-n)\rho_s C_{PS} + \theta\rho_w C_{\rho w} + (n-\theta)\rho_v C_{PV} + (n-\theta)\rho_g C_{Pg}\,, \tag{50}$$

where C_T is the specific heat capacity of the mixture.

The latent heat can be considered temperature-dependent as it has been considered by Geraminegad and Saxena[14]; since the effect of temperature on the latent heat is negligible, in this study, it is considered to be constant.

The thermomechanical coupling is done via the coupling matrix in which the term of $C = D\,D_T^{-1}$ is involved. The vector of D_T is calculated from void ratio changes under heating.

2.2.2. *Fluid and air flow properties*

The main fluid and air flow parameters are water and air permeability of porous media. The anisotropic flow water is considered in this study. It is obvious that according to the deposition manner of sediments in nature, the horizontal water permeability is usually more significant in water flow. Both water and air permeabilities depend strongly on water content and void ratio of medium. The effect of volume change of skeleton on the permeability is introduced via void ratio state surface, and the effect of water content is introduced by the degree of saturation state surface where both of them are temperature-dependent. The expression used in this study has the following form:

$$K_{wz} = K_{wzo}\left[\frac{S_r - S_{ru}}{1 - S_{ru}}\right]^b \left(\frac{\nu_r}{\nu_T}\right), \tag{51}$$

with saturated soil water permeability $K_{wzo} = a \cdot 10^{\alpha e}$, S_{ru} is residual degree of saturation, e is void ratio, S_r is degree of saturation, and a, b, and α are constants. ν_T is dynamic viscosity of water at any temperature and υ_r is dynamic viscosity at any arbitrary reference temperature.

The effect of temperature on the water permeability is introduced by considering the change of water dynamic viscosity due to temperature variations. A formula has been derived by the best fitting of the experiment values given in Gatmiri.[9] Other expressions are listed as follows:

$$\nu_T = \exp(-0.0181218T) \times 1.54158 \times 10^{-6}, \tag{52}$$

$$\nu_T = 0.6612 \times (T - 229)^{-1.562}, \tag{53}$$

$$\nu_T = 1.74 - 0.05T + 0.001T^2 - 0.0000175T^3. \tag{54}$$

Air permeability depends on suction too:

$$K_g = c\frac{\gamma_g}{\mu_g}[e(1 - S_r)]^d, \tag{55}$$

where γ_g is specific weight of gas, μ_g its viscosity, and c, d are constants. The value of μ_g according to Kaye and Laby is given as $1.846 \times 10^{-2}\,\mathrm{kPa \cdot s}$. It is assumed that heating has no effect on gas permeability.

3. Damage

Two dissipation phenomena can occur in the soils usually forming the geological barrier: plastic deformation and fracturing. Plastic strains are generated by sliding microscopic mechanisms. Material damage grows with the size of microcracks. It would thus be restrictive to identify the plastic and the damaged zones. Moreover, degraded material properties may be partially recovered by crack closure. On the contrary, plastic deformations are irreversible. It thus seems necessary to introduce new variables to model damage.

Since damage may be reversible through the healing process, it might be necessary to introduce two damage variables. To model the closure of tensile fractures

in concrete subjected to compressive stress, Frémond uses distinct damage variables for tension and compression.[17] A parallel can be drawn with elastoplastic theories involving softening. In their study of granular rock materials, Vardoulakis and Sulem define a plastic state variable to model the hardening due to friction. In addition, they introduce a back pressure acting as a confining stress to represent the softening behavior related to cohesion. In the same way, rock joint models that do not take gouge production into account overestimate dilatancy effects.

Fracturing induces strain localization. A local formulation may be inadequate to determine the size of the damaged zone and to describe the post-localization behavior. If localization occurs, static partial differential equations (PDE) may lose their ellipticity, while in dynamics, PDEs may turn nonhyperbolic. The dissipated energy tends to zero, which is physically absurd, since the damage activity increases in the softening regime. The post-localization solution depends on the mesh refinement. Therefore, it may be necessary to resort to a nonlocal or to a gradient-enhanced theory. In a nonlocal formulation, it is assumed that the damage computed at one material point also affects its neighbors. The extent of this zone of influence determines the size of a unit cell whose characteristic dimension is defined as an internal material length. A homogenization on the unit cells provides the macroscopic stresses and strains. The weighting functions may include parameters controlling the size of the set of integration points used in the averaging process. The main difficulty of this technique is to find realistic values for the material internal length and the controlling parameter. A second regularization method consists in introducing the gradient of the state variables. It has been used in plasticity frameworks,[17] and in plasticity models coupled to damage. In these formulations, the free energy generally depends not only on strain and damage, but also on the strain gradient and the damage gradient. Material length may appear when the theoretical framework is based on the development of averaged quantities in Taylor series. The introduction of gradients imposes stronger regularity requirements in the weak formulation used in the finite element method.

Four options may be adopted: a micromechanical approach, a phenomenological model, a formulation combining micromechanical and phenomenological considerations, and a representation of damage based on the introduction of specific damage and healing strains. Introducing specific deformations dedicated to the modeling of damage and healing is perhaps the easiest way to introduce fracturing in the model implemented in θ-Stock. Indeed, the THHM elastoplastic model is based on an additive breakdown of strains, involving plasticity terms due to suction and temperature. Like in the model of Hou,[18] damage irreversible strains and healing-related strains may be introduced. The main difficulty of this theoretical framework lies in the formulation of the yield functions, which may couple plasticity and damage processes.

The first part of this section is dedicated to the presentation of the main types of damage models available in the literature. The second part recalls the main issues related to flow models in multimodal and multicontinuum systems. The third part

examines the challenges that one has to face when modeling damage in porous media. A new thermohydromechanical damage model has been developed in Arson's thesis[19] and implemented in θ-Stock.[20] The model framework has been explained in Refs. 21–23. In the fourth part of this section, a numerical simulation resorting to this model is presented.

3.1. *Types of models*

3.1.1. *Micromechanical models*

The micromechanical approach consists in modeling the influence of local damage on the macromechanical behavior. Damage variables have a physical meaning related to the degradation of elastic properties or to the characteristics of the fracture network. It is assumed that stresses are redistributed due to a decrease is the effective material area.

Generally, effective stresses are defined by means of an effective stress operator[24]:

$$\underline{\underline{\hat{\sigma}}} = \underline{\underline{\underline{\underline{M}}}}(\Omega) : \underline{\underline{\sigma}}\,, \tag{56}$$

where the damage variable Ω can be a tensor. For second-order damage variables, the effective stress operator of Courdebois and Sidoroff is often adopted:

$$\underline{\underline{\hat{\sigma}}} = \underline{\underline{\underline{\underline{M}}}}(\underline{\underline{\Omega}}) : \underline{\underline{\sigma}} = (\underline{\underline{\underline{\underline{Id}}}} - \underline{\underline{\Omega}})^{-1/2} \cdot \underline{\underline{\sigma}} \cdot (\underline{\underline{\underline{\underline{Id}}}} - \underline{\underline{\Omega}})^{-1/2}\,. \tag{57}$$

The effective stress concept is often combined to the principle of equivalent elastic energy (PEEE) to compute the damaged rigidity tensor $\underline{\underline{\underline{\underline{D_e}}}}(\underline{\underline{\Omega}})$. This approach consists in postulating that the elastic energy of the intact material subjected to the effective stress $\underline{\underline{\hat{\sigma}}}$ is equal to the elastic energy of the damaged material subjected to the real stress $\underline{\underline{\sigma}}$:

$$W_e(\underline{\underline{\hat{\sigma}}}, \Omega = 0) = W_e(\underline{\underline{\sigma}}, \Omega)\,. \tag{58}$$

The development of equality (58) results in

$$\frac{1}{2}\underline{\underline{\sigma}}^T : (\underline{\underline{\underline{\underline{D_e}}}}(\Omega))^{-1} : \underline{\underline{\sigma}} = \frac{1}{2}\underline{\underline{\sigma}}^T : \underline{\underline{\underline{\underline{M}}}}(\Omega)^T : (\underline{\underline{\underline{\underline{D_e^0}}}})^{-1} : \underline{\underline{\underline{\underline{M}}}}(\Omega) : \underline{\underline{\sigma}}\,, \tag{59}$$

$$\underline{\underline{\underline{\underline{D_e}}}}(\Omega) = \underline{\underline{\underline{\underline{M}}}}(\Omega)^{-1} : \underline{\underline{\underline{\underline{D_e^0}}}} : \underline{\underline{\underline{\underline{M}}}}(\Omega)^{-T}\,. \tag{60}$$

The definition of an effective stress provides a framework to determine the damaged mechanical properties of the material. However, damage remains an abstract notion, represented by its influence on behavior laws.

In many models, cracks of close orientations are gathered in *families*. Supposing for example that the material is fractured in three principal directions $\underline{n_i}$, the

damage variable can be written as a diagonal tensor whose eigenvalues d_i represent crack densities:

$$\underline{\underline{\Omega}} = \sum_{i=1}^{3} d_i \underline{n_i} \otimes \underline{n_i} \,. \tag{61}$$

The crack density d_i depends on the number of cracks belonging to the ith family and on the radii of each of these cracks. In hydromechanical problems, it is often useful to define the characteristic crack opening e. Shao and his coworkers[25] considered that if k fractures damaged the representative volume element in all the possible directions $\underline{n}$ of space, the irreversible strain caused by damage should be

$$\underline{\underline{\varepsilon}}^d = \frac{k}{4\pi . V_{\text{REV}}} \int_{S_{\text{REV}}} \pi e(\underline{n}) r(\underline{n})^2 \underline{n} \otimes n dS \,. \tag{62}$$

In expression (62), the $1/4\pi$ coefficient indicates that the surface integral is scaled by the solid angle Bazant[26] proposed to take fracture interactions into account by defining crack opening as a function of the energy release rates F_j of every crack of the REV, weighed by interaction coefficients λ_{ij} specific to each couple of fractures:

$$e_i = \sum_{j=1}^{k} \lambda_{ij} F_j \,. \tag{63}$$

3.1.2. *Energetic approaches*

Energetic considerations are particularly suited to model dissipative phenomena such as damage and plasticity. Thermodynamic potentials are given specific forms. The resolution of the problem of maximum dissipation makes it possible to deduce the behavior, flowing, and hardening/softening laws. The model is thus automatically thermodynamically consistent.

3.1.3. *Thermodynamic framework*

At a local point $\underline{x}$, the internal energy U of the studied system depends on entropy $S(\underline{x})$, strain variables $\underline{\underline{E}}(\underline{x})$, and on parameters representing irreversible or dissipative processes $\nu_i(\underline{x})$. The first law of thermodynamics means that the variation of the internal energy is equal to the work of deformation diminished of the heat provided to the exterior of the system:

$$\dot{U}(S(\underline{x}), \underline{\underline{E}}(\underline{x}), \upsilon_i(\underline{x})) = \underline{\underline{\Sigma}}(\underline{x}) : \underline{\underline{\dot{E}(\underline{x})}} - \underline{\nabla} \cdot \underline{q}(\underline{x}) \,. \tag{64}$$

$\underline{\underline{\Sigma}}(\underline{x})$ is the generalized stress tensor and $\underline{q}(\underline{x})$ is the heat flux vector. Due to the occurrence of irreversible processes, entropy production always exceeds the quantity of heat transmitted to the exterior:

$$T(\underline{x}) \dot{S}(\underline{x}) \geq -\underline{\nabla} \cdot \underline{q}(\underline{x}) \,, \tag{65}$$

where $T(\underline{x})$ is the temperature of the medium. Combining Eqs. (64) and (65) leads to the Clausius–Duhem Inequality (CDI):

$$T(\underline{x})\dot{S}(\underline{x}) \geq \dot{U}(S(\underline{x}), \quad \underline{\underline{E}}(\underline{x}), \upsilon_i(\underline{x})) - \underline{\underline{\Sigma}}(\underline{x}) : \underline{\underline{\dot{E}}}(\underline{x})\,. \tag{66}$$

The partial Legendre transform of the internal energy relatively to entropy is defined as the Helmholtz free energy $F(T(\underline{x}), \underline{\underline{E}}(\underline{x}), \upsilon_i(\underline{x}))$:

$$U(S(\underline{x})), \underline{\underline{E}}(\underline{x}), \upsilon_i(\underline{x})) - F(T(\underline{x}), \underline{\underline{E}}(\underline{x}), \upsilon_i(\underline{x})) = T(\underline{x})S(\underline{x})\,, \tag{67}$$

$$\begin{aligned} T(\underline{x}) &= \frac{\partial U(S(\underline{x}), \underline{\underline{E}}(\underline{x}), \upsilon_i(\underline{x}))}{\partial S(\underline{x})}\,, \\ S(\underline{x}) &= -\frac{\partial F(T(\underline{x}), \underline{\underline{E}}(\underline{x}), \upsilon_i(\underline{x}))}{\partial T(\underline{x})}\,. \end{aligned} \tag{68}$$

The free energy of Gibbs $G(T(\underline{x}), \underline{\underline{\Sigma}}(\underline{x}), \upsilon_i(\underline{x}))$ is the partial Legendre transform of the free Helmholtz energy relatively to the strain variable:

$$F(T(\underline{x}), \quad \underline{\underline{E}}(\underline{x}), \quad \upsilon_i(\underline{x})) + G(T(\underline{x}), \quad \underline{\underline{\Sigma}}(\underline{x}), \quad \upsilon_i(\underline{x})) = \underline{\underline{\Sigma}}(\underline{x}) : \underline{\underline{E}}(\underline{x})\,, \tag{69}$$

$$\underline{\underline{\Sigma}}(\underline{x}) = \frac{\partial U(S(\underline{x}), \underline{\underline{E}}(\underline{x}), \upsilon_i(\underline{x}))}{\partial \underline{\underline{E}}(\underline{x})} = \frac{\partial F(T(\underline{x}), \underline{\underline{E}}(\underline{x}), \upsilon_i(\underline{x}))}{\partial \underline{\underline{E}}(\underline{x})}\,, \tag{70}$$

$$\underline{\underline{E}}(\underline{x}) = \frac{\partial G(T(\underline{x}), \underline{\underline{\Sigma}}(\underline{x}), \upsilon_i(\underline{x}))}{\partial \underline{\underline{\Sigma}}(\underline{x})} = -\frac{\partial U(S(\underline{x}), \underline{\underline{\Sigma}}(\underline{x}), \upsilon_i(\underline{x}))}{\partial \underline{\underline{\Sigma}}(\underline{x})}\,. \tag{71}$$

3.2. *Hydraulic properties of an undamaged porous medium*

Many flow theories are based on van Genuchten–Mualem model.[27] To represent the global hydraulic behavior of the representative elementary volume (REV), an equivalent medium has to be defined. The equivalent hydraulic properties of the REV are deduced from a homogenization technique.

Using van Genuchten–Mualem model we study that the fractured porous medium amounts to considering that cracks and matrix pores are all connected and form a unique network, of space-variable pore size. Moreover, a Bell-type relation is assumed between the nondimensional water content $\theta(h)$ and pressure head h:

$$\theta(h) = [1 + (\alpha h)^n]^{-m}\,, \tag{72}$$

in which the nondimensional water content is defined as

$$\theta(h) = \frac{\theta_w(h) - \theta_{wr}}{\theta_{ws} - \theta_{wr}}\,. \tag{73}$$

θ_{wr} and θ_{ws} are the residual and satiated water contents, respectively. α is the pore size for which pore density is maximal. The α parameter thus gives an idea of the more frequent pore size characterizing the material. m and n control the

distribution extent toward a fine or coarse medium. Resorting to Mualem's integral formula, the relative water permeability is defined as

$$k_R(\theta(h)) = [\theta(h)]^{1/2} \left[\frac{\displaystyle\int_0^{\Theta(h)} \frac{1}{h(x)} dx}{\displaystyle\int_0^1 \frac{1}{h(x)} dx} \right]^2 . \tag{74}$$

The integration scheme imposes that

$$m = 1 - \frac{1}{n}, \quad 0 < m < 1 . \tag{75}$$

Taking the inverse of relation (74) leads to

$$k_R(\theta(h)) = [\theta(h)]^{1/2} [1 - (1 - [\theta(h)]^{1/m})^m]^2 . \tag{76}$$

3.3. *Hydromechanical couplings in a fractured porous medium*

Continuum damage mechanics describes the degraded mechanical behavior of the rock mass. Flow network theories predict water transfers, considering hydraulic parameters only. The main issue in modeling the excavation damaged zone (EDZ) is thus to combine hydromechanical and damage concepts in a single theory. The aim of the following section is to propose a fully coupled hydromechanical damage model, which would be in conformity with the formulation adopted in θ-Stock.

3.3.1. *Introducing damage in hydraulic properties*

Some damage models introduce a damage dependency in the expression of permeability.[25,28] But the given formulas generally involve mechanical parameters only. In fact, the computed permeability reduces to the intrinsic component of absolute permeability. It is possible to define the absolute permeability of an unsaturated damaged medium as the product of a damaged intrinsic permeability with a van Genuchten–Mualem type relative permeability[27]:

$$\underline{\underline{K}}^{\text{abs}}(\underline{\varepsilon}, \underline{\Omega}, \theta) = k^{\text{rel}}(\theta)\, \underline{\underline{k}}^{\text{int}}(\underline{\varepsilon}, \underline{\Omega}) . \tag{77}$$

The relative permeability $k^{\text{rel}}(\theta)$ is only related to interstitial fluids, and does not depend on damage. The intrinsic permeability $\underline{\underline{k}}^{\text{int}}(\underline{\varepsilon}, \underline{\Omega})$ characterizes the damaged solid part of the medium, and takes irreversible fracturing and path orientation into account. In θ-Stock, the strain dependency falls down to a porosity (n) dependency. For an undamaged unsaturated material subjected to isothermal conditions, the intrinsic permeability is defined as

$$\underline{\underline{k}}^{\text{int}}(n, \Omega = 0) = k_0 \cdot 10^{\alpha_k \cdot e}\, \underline{\underline{Id}} , \tag{78}$$

k_0 is a reference permeability and α_k is a material parameter. e is the void ratio, defined by a state surface depending on stress and suction.[1]

To extend the model to a damaged unsaturated material, it is proposed to split the intrinsic permeability as follows:

$$\underline{\underline{k^{\text{int}}}}(n, \underline{\underline{\Omega}}) = \underline{\underline{k_1}}(n^{\text{rev}}, \underline{\underline{\Omega}}) + \underline{\underline{k_2}}(n^{\text{frac}}, \underline{\underline{\Omega}}) \,, \tag{79}$$

where n^{rev} represents the reversible evolution of volumetric deformations, including crack closing. As the damage model induces a dependency between strains and damage, the reversible component of the intrinsic permeability $\underline{\underline{k_1}}$ depends not only on reversible porosity n^{rev}, but also on damage $\underline{\underline{\Omega}}$. By analogy with the formulas adopted in θ-Stock, the following expression is chosen:

$$\underline{\underline{k_1}}(n^{\text{rev}}, \underline{\underline{\Omega}}) = k_0 \cdot 10^{\alpha_k \cdot e^{\text{rev}}} \underline{\underline{Id}} \,, \tag{80}$$

where e^{rev} is the void ratio deduced from the computation of reversible deformations. n^{frac} refers to the porosity generated by fracturing. Damage is defined by means of a formula similar to expression (61). It is thus assumed that three main families of cracks damage the REV chosen to study the bedrock. Following the reasoning of Shao and his coworkers,[25] it is supposed that cracks are penny-shaped planes of radius r_k, of opening e_k, and of normal direction $\underline{n_k}$, in which the interstitial liquid flows in the direction parallel to the plane. Applying the Navier–Stokes formulas to compute the celerity of the flow in the fracture network ($\underline{v_w^{\text{frac}}}$) provides

$$\underline{v_w^{\text{frac}}} = -\left(\frac{1}{12\mu_w} \cdot \frac{\pi}{a^3} \cdot \sum_{k=1}^{3} r_k^2 \cdot e_k^3 \cdot (\underline{\underline{\delta}} - \underline{n_k} \otimes \underline{n_k}) \right) \cdot \underline{\nabla} p_w \,, \tag{81}$$

μ_w is the dynamic viscosity of the interstitial liquid, a is the characteristic dimension of the REV, and p_w is the interstitial liquid pressure. Like in the other behavior models programmed in θ-Stock, the liquid transfer is assumed to be diffusive, and the Darcy law is adopted:

$$\underline{v_w^{\text{frac}}} = -\underline{\underline{k_2}}(n^{\text{frac}}, \underline{\underline{\Omega}}) \cdot \underline{\nabla} \left(\frac{p_w}{\gamma_w} + z \right) , \tag{82}$$

in which γ_w is the volumetric weight of the interstitial liquid, and z denotes the vertical coordinate, oriented positively upward. Equations (81) and (82) result in the following expression for the irreversible component of the intrinsic permeability:

$$\underline{\underline{k_2}}(n^{\text{frac}}, \underline{\underline{\Omega}}) = \frac{\gamma_w}{12\mu_w} \cdot \frac{\pi}{a^3} \cdot \sum_{k=1}^{3} r_k^2 \cdot e_k^3 \cdot (\underline{\underline{\delta}} - \underline{n_k} \otimes \underline{n_k}) \,. \tag{83}$$

3.3.2. *Extending damage models to unsaturated materials*

Damage modeling in unsaturated materials is frequently based on Biot's theory. Most approaches combine a micromechanical definition of damage $\underline{\underline{\Omega}}$ with a

postulate on the expression of the free energy $F(\underline{\underline{\varepsilon}}, \underline{\underline{\Omega}})$.[25] The constitutive relation has the following general expression:

$$d\underline{\underline{\sigma}} = d\left(\frac{\partial F(\underline{\underline{\varepsilon}}, \underline{\underline{\Omega}})}{\partial \underline{\underline{\varepsilon}}}\right)_{ij} - b[S_w p_w + (1 - S_w)p_g] \cdot \underline{\underline{Id}}\,. \tag{84}$$

b is Biot's hydromechanical coupling parameter, p_g is the gas pressure, and S_w denotes the liquid saturation degree. Adopting such a representation of stress makes it possible to uncouple poromechanical and damage effects in the constitutive stress relation. Capillarity effects on deformation are neglected. Damage growth is yet synonymous of fracturing increase. Defect initiation or crack aperture generates a rise of pore size at the scale of the global network of the equivalent medium. Bigger pores induce smaller capillarity effects, and consequently, a weaker rigidity.[3] Conversely, suction is work-conjugated to the partial porosity of the liquid phase, which originates hydraulic effects in the mechanical behavior. That is why a formulation based on net stress and suction might be more satisfying from a conceptual point of view. To the authors' knowledge, only one formulation based on net stress and suction has been proposed so far to model damage in unsaturated porous media (apart from the authors' model[19]): Lu and his coworkers[29] proposed to split total stresses $\underline{\underline{\sigma^a}}$ in a relatively damaged part $\underline{\underline{\sigma^d}}$ and a relatively intact part $\underline{\underline{\sigma^i}}$:

$$\underline{\underline{\sigma^a}} = (1 - \omega)\underline{\underline{\sigma^i}} + \omega\underline{\underline{\sigma^d}}\,. \tag{85}$$

ω is a scalar damage variable supposed to depend on suction s and deviatoric strains ε_s:

$$d\omega = \underline{\underline{L_1}}(\varepsilon_s, s) : d\underline{\underline{\varepsilon}} + L_2(\varepsilon_v, s)ds\,. \tag{86}$$

ε_v refers to volumetric strains. Contrary to a mere effective stress concept, the damaged regions of the material are still subjected to stresses, even if these damaged stresses $\underline{\underline{\sigma^d}}$ do not follow the same stress/strain relations than the undamaged stresses $\underline{\underline{\sigma^i}}$. Lu's research team assumed that the damage threshold was reached before the plastic threshold. Accordingly, they affected a nonlinear elastic behavior law to the intact stresses and an elastoplastic Barcelone-like behavior law to the damaged stresses:

$$d\underline{\underline{\sigma^i}} = \underline{\underline{\underline{\underline{D_e}}}} : d\underline{\underline{\varepsilon}} + \underline{\underline{D_{se}}}ds\,, \tag{87}$$

$$d\underline{\underline{\sigma^d}} = \underline{\underline{\underline{\underline{D_{ep}}}}} : d\underline{\underline{\varepsilon}} + \underline{\underline{D_{sep}}}ds\,, \tag{88}$$

where $\underline{\underline{\underline{\underline{D_e}}}}$ and $\underline{\underline{\underline{\underline{D_{ep}}}}}$ are respectively the elastic and elastoplastic mechanical rigidity tensors, and $\underline{\underline{\underline{\underline{D_{se}}}}}$ and $\underline{\underline{\underline{\underline{D_{sep}}}}}$ are respectively the elastic and elastoplastic suction rigidity tensors. Considering Eq. (85), the evolution of total stresses writes

$$d\underline{\underline{\sigma^a}} = (1 - \omega)d\underline{\underline{\sigma^i}} + \omega d\underline{\underline{\sigma^d}} + \underline{\underline{\sigma^r}}d\omega\,, \tag{89}$$

in which the stress difference $\underline{\underline{\sigma^r}} = \underline{\underline{\sigma^d}} - \underline{\underline{\sigma^i}}$ represents the transition between relatively intact and relatively broken states. The increment of total stress is determined by combining Eqs. (86)–(89). Supposing that strain and suction change consistently during loading in the relatively intact and relatively damaged regions, it is possible to simplify the constitutive relation into a general expression of the type:

$$d\underline{\underline{\sigma^a}} = \underline{\underline{\underline{\underline{D_{edmg}}}}} : d\underline{\underline{\varepsilon}} + \underline{\underline{D_{sdmg}}} ds \,. \tag{90}$$

$\underline{\underline{\underline{\underline{D_{edmg}}}}}$ and D_{sdmg} denote the elastoplasticity damage rigidity tensors associated with strain and suction respectively. The model of Lu and his coworkers[29] can easily be extended to anisotropic damage. However, the approach is merely micromechanical and thermodynamic requirements are not considered.

In θ-Stock, the behavior laws of unsaturated media are formulated in net stress $\underline{\underline{\sigma'}} = \underline{\underline{\sigma}} - p_g \cdot \underline{\underline{Id}}$ and suction $s = p_g - p_w$. Corresponding to the chosen stress state variables, strain components are defined as follows[2,3]:

$$\begin{cases} d\underline{\underline{\varepsilon}} = d\underline{\underline{\varepsilon_M}} + d\underline{\underline{\varepsilon_S}} \,, \\ d\underline{\underline{\varepsilon_M}} = \underline{\underline{\underline{\underline{D_e}}}}^{-1} : d\underline{\underline{\sigma'}} \,, \\ d\underline{\underline{\varepsilon_S}} = \underline{\underline{D_s}}^{-1} \cdot ds \,, \end{cases} \tag{91}$$

$\underline{\underline{\underline{\underline{D_e}}}}$ is the standard stiffness tensor, and $\underline{\underline{D_s}}$ is defined as a rigidity associated to suction. To adapt this breakdown to damage modeling, an inelastic deformation $\underline{\underline{\varepsilon^d}}$ related to damage has to be added, and it is assumed that the elastic strains also depend on damage:

$$\begin{cases} d\underline{\underline{\varepsilon}} = d\underline{\underline{\varepsilon^e_M}} + d\underline{\underline{\varepsilon^e_S}} + d\underline{\underline{\varepsilon^d}} \,, \\ d\underline{\underline{\varepsilon^e_M}} = \underline{\underline{\underline{\underline{D_e}}}}(\underline{\underline{\Omega}})^{-1} : d\underline{\underline{\sigma'}} \,, \\ d\underline{\underline{\varepsilon^e_S}} = \underline{\underline{D_s}}(\underline{\underline{\Omega}})^{-1} \cdot ds \,. \end{cases} \tag{92}$$

The elastic strains are known if the damaged rigidities $\underline{\underline{\underline{\underline{D_e}}}}(\underline{\underline{\Omega}})$ and $\underline{\underline{D_s}}(\underline{\underline{\Omega}})$ are known. Damaged stress variables may be defined for net stress and suction,[22] by resorting to Cordebois and Sidoroff operator (Eq. (57)). Then, applying the principle of equivalent elastic energy for the mechanical deformation energy and the capillary deformation energy makes it possible to compute $\underline{\underline{\underline{\underline{D_e}}}}(\underline{\underline{\Omega}})$ and $\underline{\underline{D_s}}(\underline{\underline{\Omega}})$.[22] To get the inelastic strain component, it is necessary to express $\underline{\underline{\varepsilon_M}}$ explicitly, which implies getting the corresponding stress/strain relationship. In other words, it is necessary to postulate the form of the free energy of the solid skeleton. One way to build the model is to split damaged mechanical potentials and poroelastic potentials. This is not the choice that has been done by the authors, but such an approach has been

adopted by Shao research team.[25,30] Adapting this approach to the framework of mechanical and capillary strains, such a postulate writes:

$$\begin{cases} F(\underline{\underline{\varepsilon}}_M, \underline{\underline{\varepsilon}}^e_S, \underline{\underline{\Omega}}) = F^{ed}(\underline{\underline{\varepsilon}}_M, \underline{\underline{\Omega}}) + F^{pe}(\underline{\underline{\varepsilon}}^e_S, \underline{\underline{\Omega}}) \,, \\ d\underline{\underline{\varepsilon}} = d\underline{\underline{\varepsilon}}^e + d\underline{\underline{\varepsilon}}^d = d\underline{\underline{\varepsilon}}^e_M + d\underline{\underline{\varepsilon}}^e_S + d\underline{\underline{\varepsilon}}^d \,, \\ d\underline{\underline{\varepsilon}}_M = d\underline{\underline{\varepsilon}}^e_M + d\underline{\underline{\varepsilon}}^d \,, \end{cases} \tag{93}$$

$F^{ed}(\underline{\underline{\varepsilon}}^e_M, \underline{\underline{\Omega}})$ is related to the degraded mechanical behavior of the material, and $F^{pe}(\underline{\underline{\varepsilon}}^e_S, \underline{\underline{\Omega}})$ corresponds to the poroelastic aspect of the model. The thermodynamic conjugation relationships write:

$$\begin{cases} \sigma' = \dfrac{\partial F^{ed}(\underline{\underline{\varepsilon}}_M, \underline{\underline{\Omega}})}{\partial \underline{\underline{\varepsilon}}_M} \,, \\ s = \dfrac{dF^{pe}(\underline{\underline{\varepsilon}}^e_S, \underline{\underline{\Omega}})}{d\underline{\underline{\varepsilon}}^e_S} = \underline{\underline{D_s}}(\underline{\underline{\Omega}})^{-1} s \,, \end{cases} \tag{94}$$

$F^{ed}(\underline{\underline{\varepsilon}}_M, \underline{\underline{\Omega}})$ needs to be postulated. Once it is done, the derivation of the first equation in Eq. (94) may be combined to the second equation in Eq. (92) to set a relationship between the increment of inelastic strains and the increment of damage. The damage evolution law may be obtained by using a simple damage evolution function and resorting to an associated flow rule.[31]

Following the reasoning usually adopted in the models programmed in θ-Stock, it may be assumed that the deformation related to suction ($\underline{\underline{\varepsilon}}^e_S$) is isotropic.[3,4] It is expressed as

$$d\underline{\underline{\varepsilon}}^e_S = \beta_s(s, \underline{\underline{\Omega}})^{-1} \cdot \underline{\underline{Id}} \cdot ds \,. \tag{95}$$

The rigidity associated to suction $\underline{\underline{D_s}}(\underline{\underline{\Omega}})$ is thus represented by a scalar modulus $\beta_s(s, \underline{\underline{\Omega}})$. In fact, only the knowledge of the volumetric part $(\varepsilon^e_S)_v$ of the deformations related to suction is needed to obtain the corresponding stress/strain relationship:

$$d\underline{\underline{\varepsilon}}^e_S = \frac{1}{3} \cdot d(\varepsilon^e_S)_v \cdot \underline{\underline{Id}} = \frac{1}{3} \cdot [d(\varepsilon^e)_v - d(\varepsilon^e_M)_v] \cdot \underline{\underline{Id}} \,. \tag{96}$$

$d(\varepsilon^e_M)_v$ can be deduced from $\underline{\underline{\varepsilon}}^e_M$. The resulting expression is of the following type[3]:

$$d(\varepsilon^e_M)_v = K(\underline{\underline{\sigma'}}, \underline{\underline{\Omega}})^{-1} dp' \tag{97}$$

in which $K(\underline{\underline{\sigma'}}, \underline{\underline{\Omega}})$ is the degraded compressive modulus and p' is the mean net stress. The requirements on Gibbs free energy $G(\underline{\underline{\sigma'}}, s, \underline{\underline{\Omega}})$ reduce to a relation of the form

$$d(\varepsilon^e)_v = d\left(\frac{\partial G(p', s, \underline{\underline{\Omega}})}{\partial p'} \right) . \tag{98}$$

By analogy with the model presented by Jenab,[4] the following formula is proposed:

$$\frac{\partial G(p', s, \underline{\underline{\Omega}})}{\partial p'} = \int K(\underline{\underline{\sigma'}}, \underline{\underline{\Omega}})^{-1} dp' + \frac{k_s}{1 + e_0} \cdot \ln \left[\frac{\hat{s} + p_{\text{atm}}}{\hat{s}_g + p_{\text{atm}}} \right] . \tag{99}$$

k_s is a compression modulus associated to suction effects in the reversible domain, e_0 is the initial void ratio, and p_{atm} refers to the atmospheric pressure. A damaged suction $\hat{s}$ is defined, in the same way as damaged stresses (Eq. (56)). $\hat{s}_g$ is the biggest damaged suction ever submitted to the material. It is the equivalent of a consolidation stress. Equations (93) and (97)–(99) lead to

$$d(\varepsilon_S^e)_v = \frac{k_s}{1+e_0} \cdot \frac{1}{\hat{s}+p_{\text{atm}}} \cdot \frac{\partial \hat{s}(s, \underline{\underline{\Omega}})}{\partial s} \cdot ds\,. \tag{100}$$

As explained earlier, the expression of the damaged suction $\hat{s}(s, \underline{\underline{\Omega}})$ can be deduced from a relation of the type of Eq. (56), which enables the full calculation of expression (100). Equations (92), (96), and (100) sum up the framework of a hydromechanical damage model for unsaturated porous media that could easily be implemented in θ-Stock software.

3.4. *A heating test simulated with the THHMD model in unsaturated conditions*

The modeling framework presented in the previous paragraph is close to the developments of Gatmiri on state-surface models. Another strategy to model thermohydromechanical damage in unsaturated porous media has been proposed in Refs. 19 and 21–23. The model, (named "THHMD model") is based on the same basic assumptions on independent state variables and strain decomposition, but the free energy is split in a different way. Moreover, temperature effects are accounted for, in particular, the potential phase changes are modeled. In the sequel, a numerical application of the THHMD model is presented. This test comprises the study of thermohydraulic behavior of bentonite which is placed around the nuclear wastes as a cover. It is inspired by the works of Pintado *et al.*[32] A thermal source is installed between two cylinder-shaped bentonite samples with diameters of 38 mm and heights of 76 mm which are both wrapped in isolate foam. Since the provided geometry and loading are both symmetrical and the calculations are performed through axial symmetry, the thermal source is modeled through the boundary condition of Newman applied to the nodes of the external boundary of the sample. To consider the effects of the isolate foam, a thermal current of zero is exerted on the external lateral boundary.

Loading falls into two conditions, preliminary and boundary. The temperature at all nodes is 22 °C for the preliminary conditions while the air pressure is equal to atmospheric pressure. In case of boundary conditions, degrees of freedom are considered unbounded and there are no limiting conditions. Boundary conditions include two stages of heating and recovery. During the heating stage which lasts for 1 week, a constant temperature is applied to the top of the sample, while it is 30 °C for the bottom sections and an adiabatic process for the external sides (in order to simulate the effect of the applied isolating layer). Air cannot penetrate the external sides at this stage. Recovery stage which takes up to 7 weeks is when the heat source is shut down. During the recovery stage which lasts for 1 week, a

zero temperature is applied to the upper boundary, while it is 30 °C for the bottom sections and an adiabatic process for the external sides. The external boundaries are impenetrable to both water and air.

The lab test of Pintado *et al.* is simulated by resorting to the elastic part of the THHMD model. The results are compared to the reference experimental data published in Ref. 32 to assess the model performance in solving multiphysics problems (Figs. 1–5). The study of numerical results shows that no rise in the temperature occurs after a period of 100 h. The temperatures calculated by θ-Stock after arriving at the thermal balance are nearly similar to those measured in the tests by Pintado *et al.* Prior to the thermal balance, the calculated temperatures at each moment were lower than tests results. This difference may be justified through the selection of thermal capacity modulus of rigid framework. C_{ps} is constant in the THHMD model and it is equal to the value resulting from Pintado *et al.*'s test at 49 °C. The thermal capacity modulus at temperatures below 49 °C is much larger than the values derived from the test which shows the high thermal inertia causing slow transfer of heat. As a result, this difference is more obvious at the beginning of the test since the difference between the numerical and lab thermal capacities is much larger.

It can be concluded that the algorithm implemented in θ-Stock for the THHMD model gives satisfactory results in complex thermohydromechanical configurations. The next step is to validate the model when damage occurs. In the absence of reference data regarding cracked bentonite samples, only sensitivity analyses are

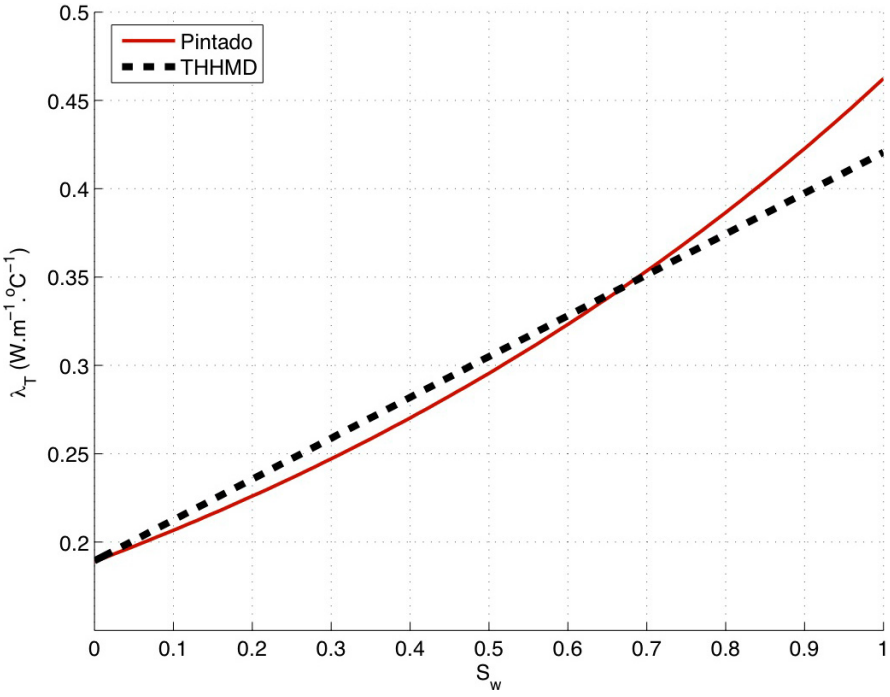

Fig. 1. Comparison of two thermal conductivity modulus.

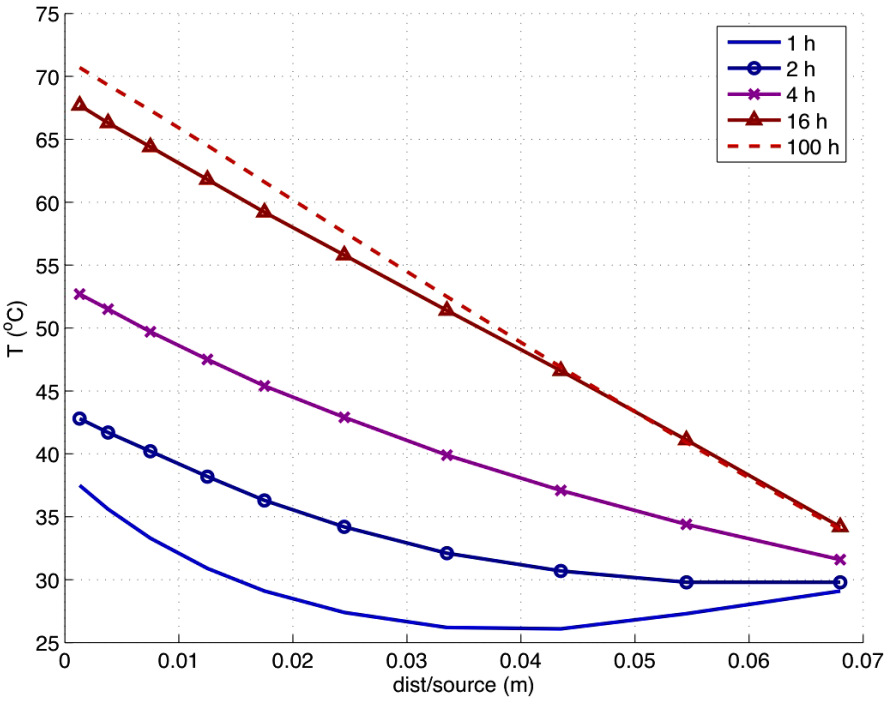

Fig. 2. Thermal contours of Pintado test — Numerical results by θ-Stock.

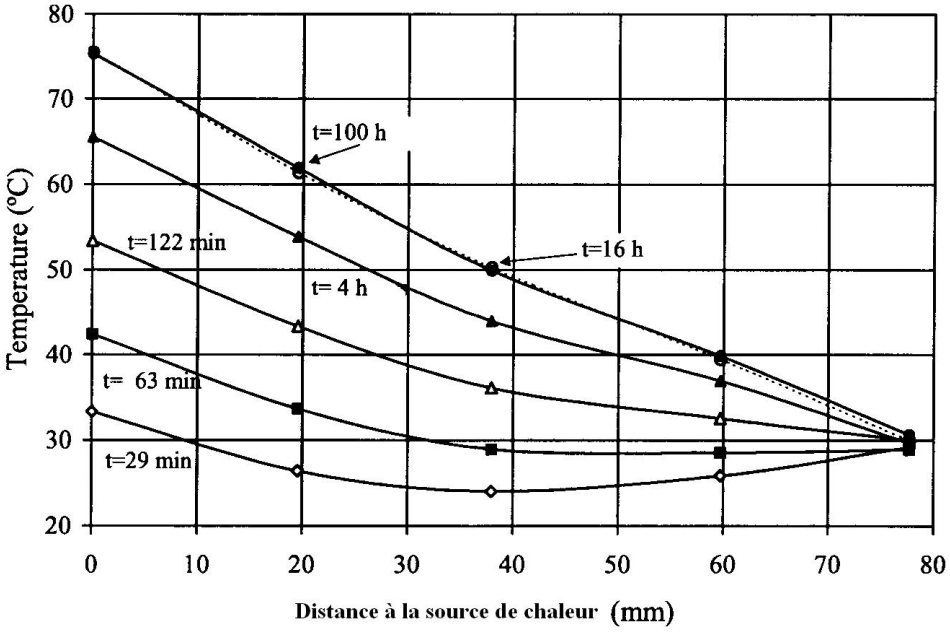

Fig. 3. Thermal contours of Pintado test — Experimental measurements.

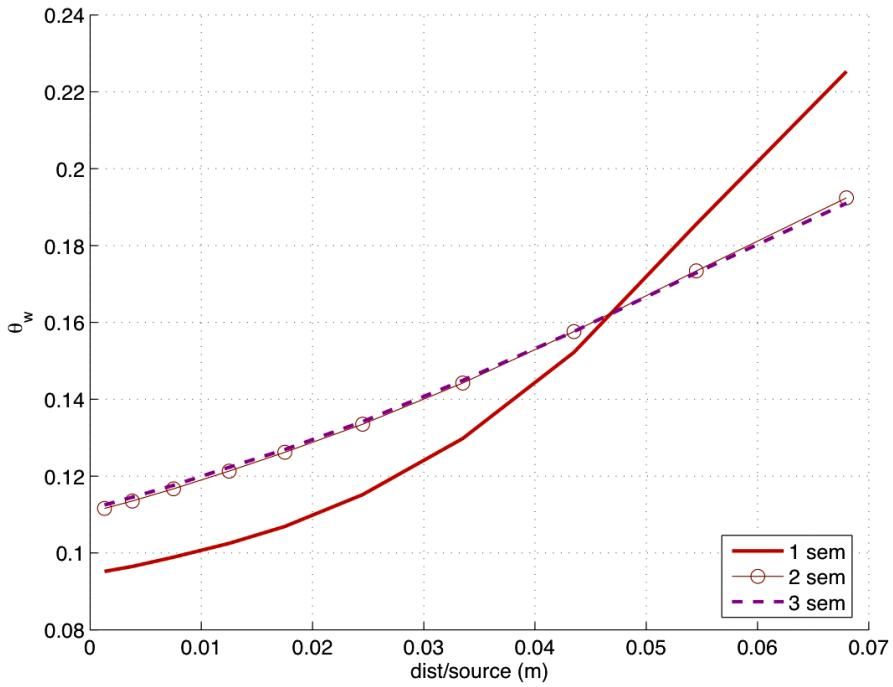

Fig. 4. Water content variations after a week of testing — Numerical results by θ-Stock.

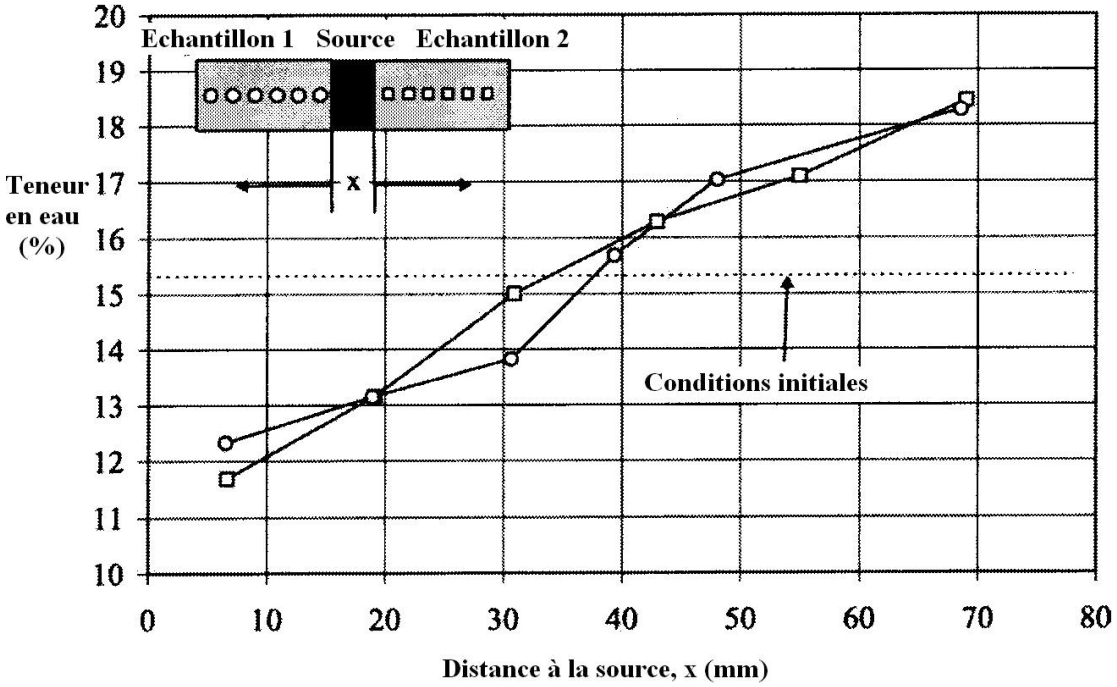

Fig. 5. Water content variations after a week of testing — Experimental measurements.

possible at this stage. Such parametric studies have already been done on less complex problems (involving temperature and pore pressure degrees of freedom only) and reported in Ref. 23.

4. Soil Surface Moisture Changes Due to Soil–Atmosphere Interaction

This part of work is based on developments done in PhD works of Hemmati in ENPC[33] and Hemmati and her coworkers.[34,35]

The computation of soil–atmosphere water fluxes (e.g., infiltration, evapotranspiration, runoff, precipitation, and interception) is required for the analysis of numerous problems in geotechnical, geoenvironmental engineering, and hydrology. Direct measurement of evapotranspiration is difficult or expensive at field scale; hence numerous equations exist to estimate it. Evapotranspiration includes evaporation of water from the soil and other surfaces and transpiration through plant stomata. Energy balance models provide a good presentation of estimating evapotranspiration, but are subject to large sensitivity to input variables, especially air temperature, humidity, and wind speed. Solar radiation plays an important role in estimating evapotranspiration. Incoming solar radiation is partially reflected, with the reminder absorbed by wetland water and vegetation. The remaining net radiation is partially intercepted by the vegetative canopy, and drives transpiration in plants. The second portion of net radiation is absorbed by wetland water, and drives evaporation. Convection and diffusion carry water away from the surface, and transfer heat from air to the wetland. Water content variations in clayey soils can give rise to significant soil deformations by shrinkage or swelling. The induced settlement is usually nonuniform and can thus result in damages to buildings, especially in case of light buildings, constructed on shallow foundations which are not adequately designed to support these differential settlements. This phenomenon is more important in long drought periods with greater changes in soil water contents. A set of equations of this part are integrated in θ-Stock by Hemmati[33] and Hemmati and her coworkers.[34,35]

4.1. *Energy balance equations*

The water transfer through soil surface occurs via two mechanisms: infiltration (positive flux) and evaporation (negative flux):

$$I_{nf} = P - (E_T + R_{off} + I_{\text{int}\,e})\,, \tag{101}$$

where I_{nf} is the infiltration, P is the precipitation, R_{off} is the runoff, E_T is surface the evapotranspiration, and $I_{\text{int}\,e}$ is the interception. The amount of precipitation, runoff, and interception are "known" inputs which can be evaluated by direct measurement at field scale.

The principle driving force for evapotranspiration (ET) is solar radiation. A good share of that radiation is converted to the latent heat of vaporization. Therefore, the

energy balance is the proper framework to interpret and predict not only evaporative processes, but also wetland water temperature. A modification of the Penman[36] approach is described. It is to be noted that there are many other versions of the energy balance. Several of these have been evaluated for green crops, because of importance of irrigation requirement in arid regions.[37]

The total energy balance equation can be expressed by

$$R_n + W_E = G + H + \lambda E_T \,, \tag{102}$$

where R_n is the net radiation, G is the soil heat, H is the sensible heat, and the term $\lambda\, E_T$ is the latent heat flux. The convective heat transfer from the soil surface to the air can be expressed by

$$H = \rho_a c_p D_{ta} \Delta T = \rho_a c_p \frac{(T_s - T_a)}{r_{ah}} \,, \tag{103}$$

where ρ_a is the air density, c_p is the specific heat of air, and r_{ah} is the aerodynamic diffusion resistance. The latent heat flux is given by

$$\lambda E_T = \frac{\lambda \varepsilon \rho_a}{p_a} D_v \, \Delta P_v = \frac{\lambda \varepsilon \rho_a}{p_a} \frac{(P_{vs} - P_{va})}{r_v} \,, \tag{104}$$

where λ is the latent heat for vaporization of water, p_a is atmospheric pressure, ε is the ratio of molecular masses of water and dry air, and r_v is vapor diffusion resistance.

Since the soil surface temperature T_s and soil surface vapor pressure P_{vs} are unknown, different methods try to solve the problem by modifying the above equations in order to make them independent of these parameters and use only the meteorological data. These simplifications may cause no problem to the evaluation of the potential evaporation in some methods such as the Penman method, but for the calculation of the actual evaporation, the effect of soil conditions like soil saturation and soil temperature should not be neglected.

4.1.1. *Net radiation in potential conditions*

Extraterrestrial radiation is depleted by the clear atmosphere and by cloud cover. The remainder reaches the soil–plants system. Plant transpiration partially intercepts it. The other portion reaches the wetland. A fraction α, the wetland albedo, of this amount is reflected. The absorbed part by the surface called net radiation is in potential condition. Net radiation in potential conditions can be obtained by

$$R_n = (1 - \alpha) R_g + \varepsilon_s \left(\varepsilon_a \, \sigma T_a^4 - \sigma \, T_{sp}^4 \right) , \tag{105}$$

where α is the surface albedo; R_g is the incoming solar radiation; ε_s is the air emissivity; σ is the Stefan–Boltzman constant; T_a is the air temperature at reference height; ε_s is the surface emissivity; and T_{sp} is the surface temperature in potential conditions.

The albedo factor is

$$\alpha = \begin{cases} 1 - \left(1 - \dfrac{\theta}{\theta_{fc}}\right)^2 & \theta \le \theta_{fc}\,, \\ 1 & \theta > \theta_{fc}\,, \end{cases} \tag{106}$$

where θ is the volumetric soil water content of the top soil layer; and θ_{fc} is the volumetric soil water content at field capacity.

4.1.2. *The convective heat transfer from the water to air and latent heat flux for vaporization*

The convective heat transfer from the water to air can be expressed by

$$H = \rho_a C_a D_{ta} \Delta T\,, \tag{107}$$

where ρ_a is the density of air; C_a is the specific heat of air; and D_{ta} is the heat diffusivity in air.

Latent heat flux for vaporization is

$$\lambda\, E_T = h_{fg} \frac{\rho_a}{P_a} \varepsilon D_v \Delta P_v\,, \tag{108}$$

where h_{fg} is the latent heat for vaporization of water; P_a is the atmospheric pressure; and ε is the ratio of molecular masses of water and dry air.

The latent heat for vaporization of water is given by

$$h_{fg} = 4.186\,(607 - 0.7\,T)\,, \tag{109}$$

where T is the water temperature.

4.1.3. *Wind energy*

Wind energy is expressed in the form

$$W_E = \frac{1}{200} \rho_a Z\, U^3\,, \tag{110}$$

where Z is the thickness of air layer, and U is the air velocity.

The value of W_E is approximately 2% of net radiation in potential conditions; hence, it can be neglected. Then Eq. (102) reduces to

$$R_n = G + H + \lambda E_T\,. \tag{111}$$

4.2. *Mass balance equations*

The net soil–atmosphere moisture flux is a function of some of the key components of the hydrology cycle, namely, precipitation, actual evaporation, runoff, and interception. The net soil–atmosphere flux may result in either infiltration (positive flux) or exfiltration (negative flux).

The total mass balance equation can be expressed by

$$I = P - (R_{off} + E + I_{\text{int}\,e})\,, \tag{112}$$

where I is infiltration; P is precipitation; R_{off} is runoff; E is surface evaporation and $I_{\text{int}\,e}$ is interception.

4.3. *Model verification*

A 17 months period of the experimental site of Mormoiron, instrumented by BRGM is modeled. Soil parameters are available from experimental tests.[38] Daily climatic data is available for Carpentras Station by Météo France. The soil settlements and soil temperature are measured by BRGM using extensometers and probes. The void ratio state surface, presented in Fig. 6, is calculated based on shrinkage curve. The degree of saturation state surface (Fig. 7) is determined using the water retention curve of the soil. Water permeability is a function of void ratio and degree of saturation. Permeability of saturated soil is considered to be about 10^{-9} m/s.

The daily meteorological data such as wind speed, air temperature, precipitation, air relative humidity, and radiation are used to calculate the boundary conditions. The calculated soil heat flux (G) as thermal boundary condition and the infiltration rate (I) as hydraulic boundary condition are presented in Figs. 8 and 9. The calculated settlements are then compared with the available *in situ* results, and good concordance can be observed in Fig. 10.

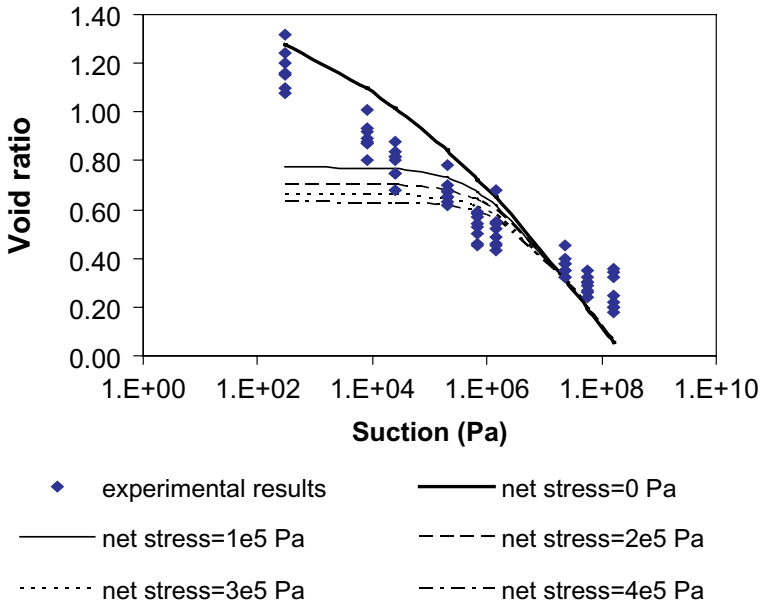

Fig. 6. Void ratio state surface.[26]

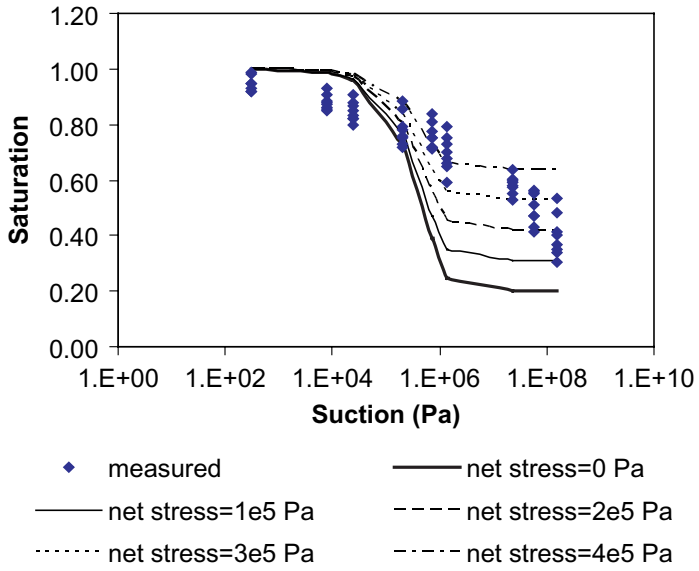

Fig. 7. Degree of saturation state surface.[26]

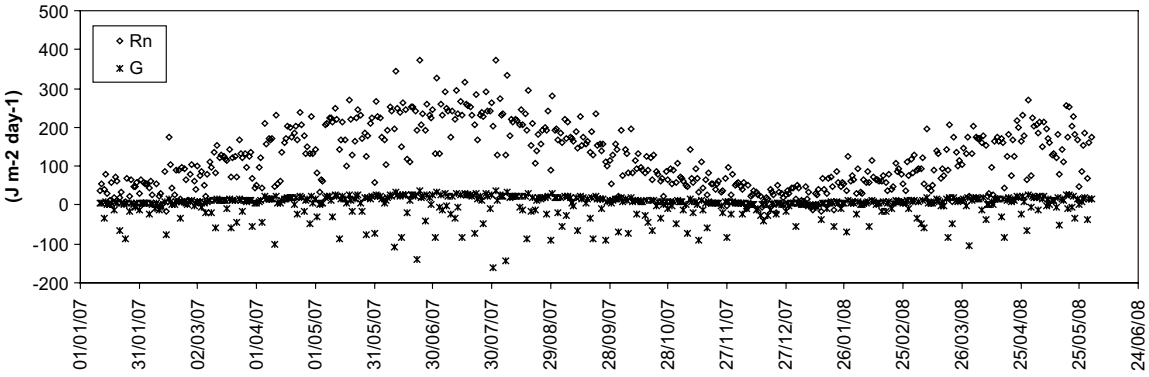

Fig. 8. Net radiation, R_n and soil heat flux, G (J m^{-2} day^{-1}).[26]

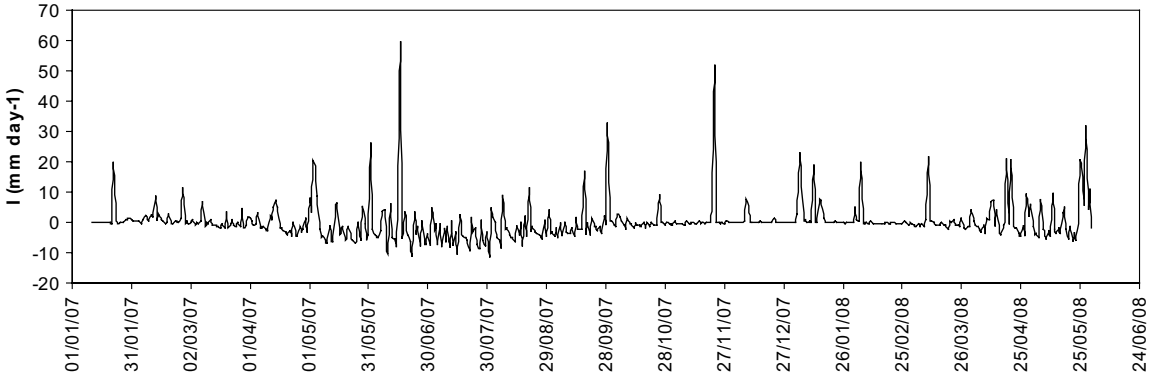

Fig. 9. Infiltration rate, I_{nf} (kg m^{-2} day^{-1}).[26]

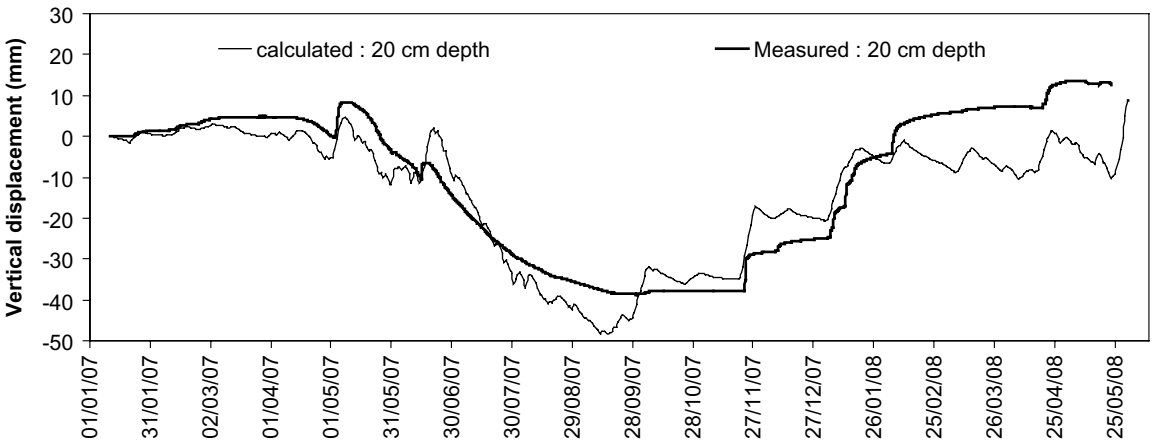

Fig. 10. Soil settlement (mm).[26]

5. Root Water Uptake Effect in Multiphase Porous Media

Roots of trees are like pumps that extract moisture from their root zone and deliver it to the atmosphere through the surface of leaves in the form of water vapor. When water demand of a tree is not met through rainfall or irrigation, it desiccates its nearby soil and creates matric suction and settlement in its root region. Moreover, it should be indicated that vegetation can have pleasant geotechnical effects too. As we noted above, root water uptake produces matric suction in the soil which increases the shear strength. This characteristic has increased the use of trees in stabilizing slopes, railways, etc. Hence, it seems necessary to study the effects of root water extraction on soils.[39]

To study the root water uptake phenomenon we need to have a set of mathematical formulas to calculate the amount of moisture that the root system can extract from the soil. There are numerous root water uptake models available in the literature. Investigators in the fields of irrigation, agriculture, soil salinization, hydrology, and soil science have been very interested to propose root water uptake models. These models can be categorized into two groups. In the first group of models, roots are assumed as individual hollow cylindrical infinite sink terms; in these models water flow is radial toward the root; the models of this group are called microscopic models. Philip seems to be the first author who suggested such a model.[11] Many other investigators tried to improve and modify his model. Nevertheless, there are some difficulties and shortages in using microscopic models; they are just applicable to steady-state water flow problems and also, it is very difficult or even impractical to quantify the characteristics of roots in such models.

These problems made investigators to think about macroscopic models — the second category, in which the root system is assumed as a unit, continuous sink term that can extract moisture nonuniformly from each differential volume of soil. This sink term should then be entered in the mass conservation equation of moisture. Gardner[40] seems to be the first to propose a macroscopic model. His model

was then extended by numerous investigators. Although macroscopic models are different in terms of the dimension of the models (1D, 2D, and 3D), the root system geometry and the root distribution function, they have the same approach. The macromechanical approach is the framework adapted in this paper to study the effect of soil–atmosphere exchange by vegetation in porous media, while the soil is unsaturated. A set of equations of this part are integrated in θ-Stock by Najari and Gatmiri.[41,42] A 2D root water uptake model is implemented and validated by Hemmati,[33] Hemmati and Gatmiri,[43] and Hemmati *et al.*[44] considering the evapotranspiration from soil surface. Evaluation of soil surface evapotranspiration is explained in Sec. 4.

5.1. *Root water uptake formulation*

To study the phenomenon of root water uptake in unsaturated soils we need to know the amount of moisture that the root system of a tree can extract from each point of the soil. Two assumptions, which are based on observations and field measurements, are applied to reach a mathematical formula that calculates the rate of root water uptake:

- The rate of root water uptake (S) in each point of the soil is proportional to the length density of root (β) in that point:
$$S_{\max}(x, y, z, t) = C_r \times \beta(x, y, z, t)\,. \tag{113}$$
It should be noted that root length density is defined as the length of root existing in each unit volume of soil (LL^{-3}).
- The amount of water that the root system uptakes can be divided into two parts: one part is used in the trees metabolism and what remains enters the atmosphere through the surface of its leaves as water vapor. The second assumption which is based on exact field measurements is that the first part of water is negligible in comparison to the second part. Thus, the whole amount of water extracted from the soil is delivered to the atmosphere.[40] Therefore, potential transpiration equals the integral of maximum rate of root water uptake on the root zone volume:
$$T_p = \int S_{\max}(x, y, z, t)dv\,. \tag{114}$$

By entering Eq. (113) in Eq. (114), we have

$$T_p = \int C_r \beta(x, y, z, t)dv = C_r \int \beta(x, y, z, t)dv\,, \tag{115}$$

$$C_r = \frac{T_p}{\displaystyle\int \beta(x, y, z, t)dv}\,, \tag{116}$$

$$\Rightarrow S_{\max}(x, y, z, t) = \frac{\beta(x, y, z, t)}{\displaystyle\int \beta(x, y, z, t)dv} T_p\,, \tag{117}$$

$$S_{\max}(x, y, z, t) = D(\beta) \times T_p\,, \tag{118}$$

in which $D(\beta)$ is called distribution function. Hence, we reached a relationship (Eq. (118)) to calculate the rate of root water uptake in each point of the root zone, while the soil does not restrict the water availability.

There are different assumptions for the shape of root zone in the literature. Some researchers assume the root zone cylindrical, while some others like Indraratna *et al.*[39] assume it as an inverted cone. The formula which is proposed by the authors of this study is

$$\left(\frac{z}{z_{\max}}\right)^{\xi} + \left(\frac{r}{r_{\max}}\right)^{\xi} = 1\,, \tag{119}$$

where $z_{\max}$ is the maximum depth of root in the soil, and $r_{\max}$ is the maximum radial distance of root from the tree trunk. For $\xi = 1$, Eq. (119) becomes an inverted cone. Also, when $\xi \to \infty$, the relationship becomes cylindrical. Thus, ξ is used to model the real shape of root region for each type of tree. The shapes of root zone for four different values of ξ are depicted in Fig. 11.

There are different propositions for root length density (β). Feddes *et al.*[45] assumed β constant in his one-dimensional simulation:

$$D(\beta) = \frac{\beta_0}{\displaystyle\int_0^{z_{\max}} \beta_0 dz} = \frac{\beta_0}{\beta_0 z_{\max}} = \frac{1}{z_{\max}}\,. \tag{120}$$

Prasad[46] proposed a linear relationship for root length density:

$$D(\beta) = \frac{\alpha(z_{\max} - z)}{\displaystyle\int_0^{z_{\max}} \alpha(z_{\max} - z) dz} = 2\left(\frac{1}{z_{\max}} - \frac{z}{z_{\max}^2}\right). \tag{121}$$

He finally concluded that using the linear relationship is not suitable for a representative modeling. However, some other investigators proposed exponential relationships for the change of root length density in depth:

$$\beta(z,t) = \beta_{\max} e^{-fz} \Rightarrow D(\beta) = \frac{\beta_{\max} e^{-fz}}{\displaystyle\int_0^{z_{\max}} \beta_{\max} e^{-fz} dz} = \frac{e^{-fz}}{\displaystyle\int_0^{Z_{\max}} e^{-fz} dz}\,. \tag{122}$$

It has been found that exponential relationships give better results. Therefore, in this paper an exponential relationship for root length density is chosen.

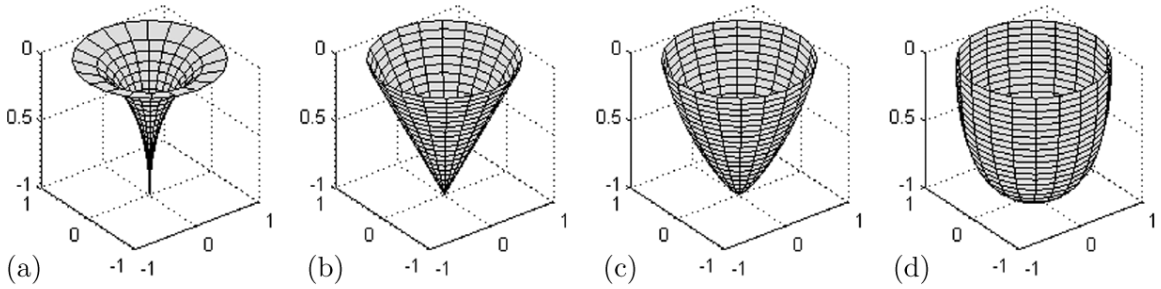

Fig. 11. Different normalized shapes of rooting zone: (a) $\xi = 0.6$; (b) $\xi = 1$; (c) $\xi = 2$; and (d) $\xi = 5$.

When a single tree is planted in a homogeneous soil, the problem is axisymmetric. In this situation, using exponential relationship for root length density variation in r and z directions, the rate of maximum root water uptake can be calculated from

$$\beta(r,z,t) = e^{-k_z|z-z_0|-k_r|r-r_0|} \Rightarrow S_{\max}(r,z,t) = \frac{e^{-k_z|z-z_0|-k_r|r-r_0|}}{\displaystyle\int_V e^{-k_z|z-z_0|-k_r|r-r_0|}dv} T_p\,, \quad (123)$$

where k_1 is a constant controlling the root length density variation in z-direction and k_2 is a constant determining the radial root length density distribution. Furthermore, (r_0, z_0) is the coordinate of the point in which the maximum root length density exists:

$$\nabla S_{\max}(r,z,t)|_{r=r_0,z=z_0} = 0\,. \quad (124)$$

Potential transpiration (T_p) is a meteorological parameter which is always reported in m/s, while this parameter should be entered as m^3/s in Eq. (129). Therefore, we should multiply T_p by πR^2, where R is the radius of foliage of the tree. The value of R is as much as $r_{\max}$ when the soil is homogeneous and there is no water restriction. The parameter $r_{\max}$ is a very good estimation of the parameter R. Moreover, in the above formula, the rate of root water uptake does not become zero at the boundary of the root zone. This problem can enter error in the calculations. In order to correct the two mentioned problems we modify Eq. (123) as below:

$$S_{\max}(r,z,t) = \frac{e^{-k_z|z-z_0|-k_r|r-r_0|}\left(1-\left(\dfrac{z}{z_{\max}}\right)^{\xi}-\left(\dfrac{r}{r_{\max}}\right)^{\xi}\right)}{\displaystyle\iiint_V e^{-k_z|z-z_0|-k_r|r-r_0|}\left(1-\left(\frac{z}{z_{\max}}\right)^{\xi}-\left(\frac{r}{r_{\max}}\right)^{\xi}\right) r d\theta r\,dx\,dz} \times \pi R^2 \times T_p\,. \quad (125)$$

When we have a row of trees, the problem becomes two-dimensional plane strain and the rate of root water uptake would be

$$S_{\max}(x,z,t) = \frac{e^{-k_z|z-z_0|-k_x|x-x_0|}\left(1-\left(\dfrac{z}{z_{\max}}\right)^{\xi}-\left(\dfrac{x}{x_{\max}}\right)^{\xi}\right)}{\displaystyle\iint e^{-k_z|z-z_0|-k_x|x-x_0|}\left(1-\left(\frac{z}{z_{\max}}\right)^{\xi}-\left(\frac{x}{x_{\max}}\right)^{\xi}\right) dx\,dz} \times 2R \times T_p\,. \quad (126)$$

5.2. *The restricting effect of soil suction on root water uptake*

The equations for the rate of root water uptake, which are presented above, are valid while there is no water deficiency for the tree. When the amount of water for the tree is restricted, root water uptake makes the soil unsaturated and matric suction is produced. This matric suction reduces the water-absorption capability of

the root. This is a completely known and fully investigated phenomenon and there are various relationships in the literature to take it into account. The relationship proposed by Feddes *et al.*[47] is more common and easier to use. Furthermore, it is validated by numerous investigators and has become classic in this field of study; therefore, we have chosen it to use in this study. Hence, the real value of S becomes

$$S(x, y, z, t) = S_{\max}(x, y, z, t) \times f(\psi)\,, \tag{127}$$

where $f(\psi)$ is called the reduction factor:

$$f(\psi) = \begin{cases} 0 & \psi < \psi_{an}\,, \\ 1 & \psi_{an} < \psi < \psi_d\,, \\ \dfrac{\psi_w - \psi}{\psi_w - \psi_d} & \psi_d < \psi < \psi_w\,, \\ 0 & \psi_w < \psi\,. \end{cases} \tag{128}$$

This reduction factor is depicted in Fig. 12; ψ_n and ψ_d are respectively the minimum and maximum matric suctions between which the water extraction takes place without any restriction. Also, ψ_w is the wilting point matric suction where the root water uptake is not available for values greater than it. The range of wilting point matric suction is 1.55–3.1 MPa.

5.3. *Potential transpiration rate*

To calculate the rate of potential transpiration T_p of a type of tree, first we should calculate the reference evapotranspiration of a 12 cm tall grass (ET_0) from Penman–Montieth formulation in that region. The parameters that are used to calculate this item are: maximum and minimum daily temperatures, daily due point temperature,

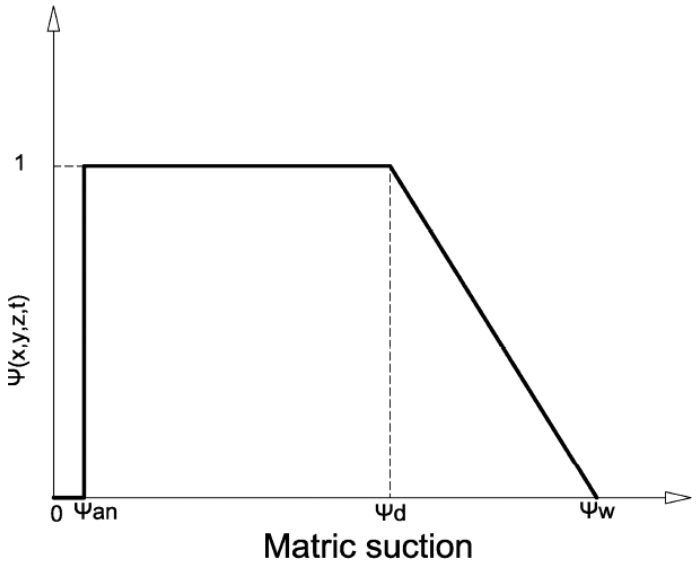

Fig. 12. Reduction factor function (restricting effect of soil suction on root water uptake).

solar radiation on grass, wind velocity at 2 m height, albedo, the day of year, and elevation. Then we should multiply ET_0 into basal crop coefficient (K_{cb}) to calculate potential transpiration rate of our specific vegetation (T_p):

$$T_p = K_{cb} ET_0 \,. \tag{129}$$

Reference crop coefficient (K_{cb}) varies for each type of vegetation and for each season of the year and is reported in agricultural and irrigation references. When the vegetation loses its leaves during nongrowing period, the K_{cb} value becomes zero. The process of T_n calculation is applicable for every tree and every region around the world.

5.4. *Model verification*

To evaluate the proposed formulation, first, we model a problem which is related to the effect of water uptake of a row of trees, solved by Fredlund and Hung.[48] In this problem water is not extracted by the root zone; it is applied as water flow boundary condition. This water flow starts from 1 m depth with the value of 15 mm/day and decreases linearly to zero at 3 m depth. It is assumed that groundwater table is at 15 m depth. It should be noted that the problem is a two-dimensional plain strain condition. Also, we just need to model half of the problem due to the symmetry. In Fig. 13 the water retention curve proposed by Fredlund and Hung is given.

The water permeability relationship, Fredlund and Hung used for their unsaturated soil model, is presented below:

$$k = \frac{k_s}{1 + a\left(\dfrac{\psi}{\rho_w g}\right)^n} \,, \tag{130}$$

where a and n are 0.001 and 2, respectively. k_s which is the permeability of saturated soil is 5.79×10^{-8} m/s. The soil is a normally consolidated clay with unit initial void ratio and Poisson's ratio of 0.3.

The problem is modeled with rectangular four-noded element mesh and is solved for a one-year period with 365 equal time steps. The matric suction results of our

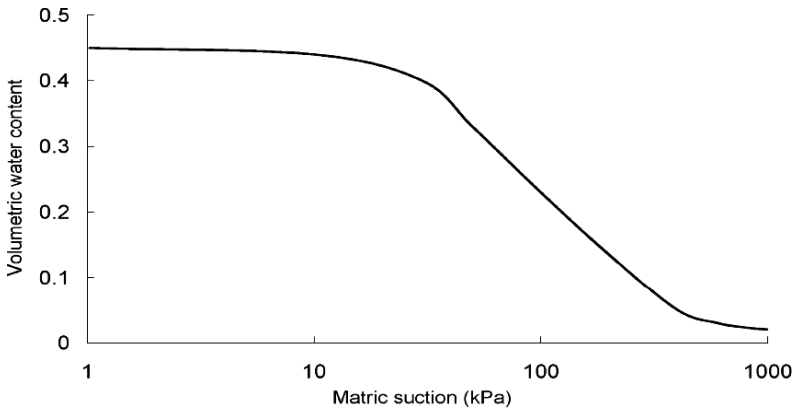

Fig. 13. Water retention curve (reproduced after Fredlund and Hung[37]).

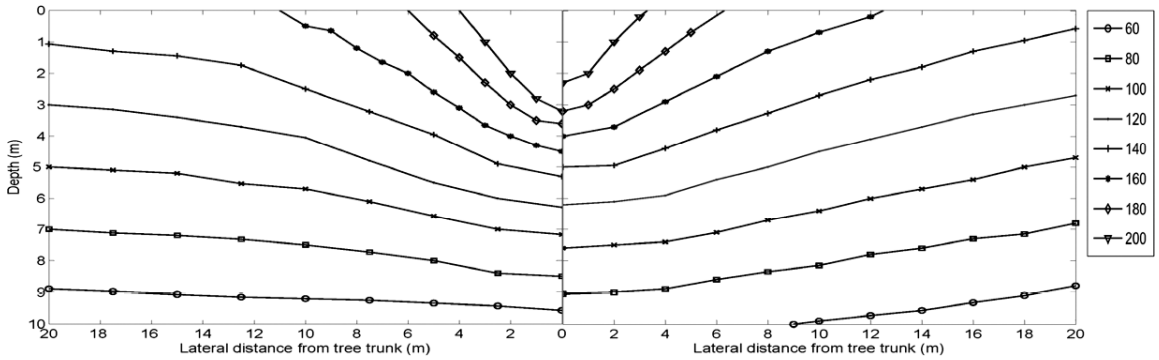

Fig. 14. Comparison of matric suction results: Reproduced after Fredlund and Hung[37] (left) and current model (right).[32]

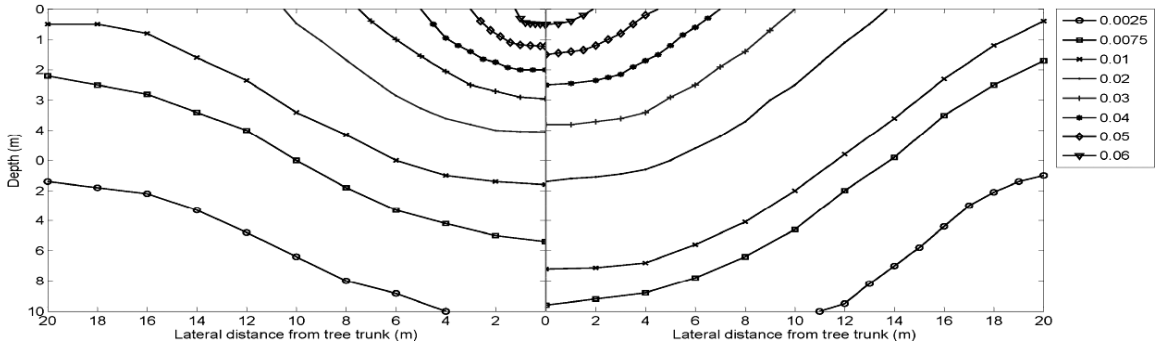

Fig. 15. Comparison of the settlement results: Reproduced after Fredlund and Hung[37] (left) and current model (right).[32]

finite element model and Fredlund and Hung simulation after one year of root water uptake are depicted in Fig. 14. Furthermore, Fig. 15 compares the settlement results of the two models. Although the unsaturated soil formulations of the two models are not the same, the results satisfactorily agree with each other. The slight disparities seen in Figs. 14 and 15 between the results of the two models are because the model proposed by Gatmiri and coworkers uses the concept of state surfaces of void ratio and degree of saturation. Moreover, θ-Stock employs Philip and de Vries' theory for heat and moisture transfer. Although many efforts have been made to the calibration of the model, this little disparity seems inevitable.

5.5. *Simulation of a single gum tree in unsaturated soil*

This problem is related to measurements done in the vicinity of a large single spotted gum tree in Holden Hill, Adelaide, by Jaksa *et al.*[49] In November 2000, some boreholes were drilled along a line on radii of 2.2, 5, 10, and 20 m, up to the depth of 4 m. Specimens were taken out from each 0.5 m depth interval. These specimens were used to measure total suction with transistor psychrometer technique. Also, the moisture content of specimens was measured, using oven drying method. The whole results are presented by Jaksa *et al.*[49]

Table 1. Values of the parameters used in the simulation of the single gum tree.[30]

Parameter	Value	Comments
T_p	9 mm/day	After Indraratna *et al.*
$r_{\max}$	17 m	$10 < r_{\max} < 20$
$z_{\max}$	9 m	After Indraratna *et al.*
R	15 m	After Indraratna *et al.*
r_0	8 m	Within the proposed range
z_0	3 m	After Indraratna *et al.*
K_z	8	Calibrations
K_r	5	Calibrations
ξ	3	Calibrations
ψ_{an}	4.9 kPa	After Indraratna *et al.*
ψ_d	40 kPa	After Indraratna *et al.*
ψ_w	3000 kPa	After Indraratna *et al.*

To verify the proposed formulation, the suction around the tree is modeled. Hence, the tree is let to extract water from its root region until it reaches equilibrium condition. As reported by Indraratna *et al.*,[39] the groundwater table is at 61.2 m depth. We analyze a cylinder with radius of 20 m and depth of 20 m in order to model the two-dimensional axisymmetric single tree water uptake problem (the soil is assumed to be homogeneous). We assume that the amount of water inflow equals the amount of moisture evaporated from the soil surface. The parameters used in this modeling are given in Table 1. Using the values of T_n and R we can simply calculate the amount of water that this tree can extract from the soil while there is no water restrictions; a 6.4 m^3/day discharge is very significant. Figure 16 shows the water retention curve suggested by Indraratna *et al.*[39] for the problem. Furthermore, Indraratna *et al.* suggested a relationship to calculate the soil permeability in this problem which is presented below[39]:

$$K = k_s \times S_r^3 \,, \tag{131}$$

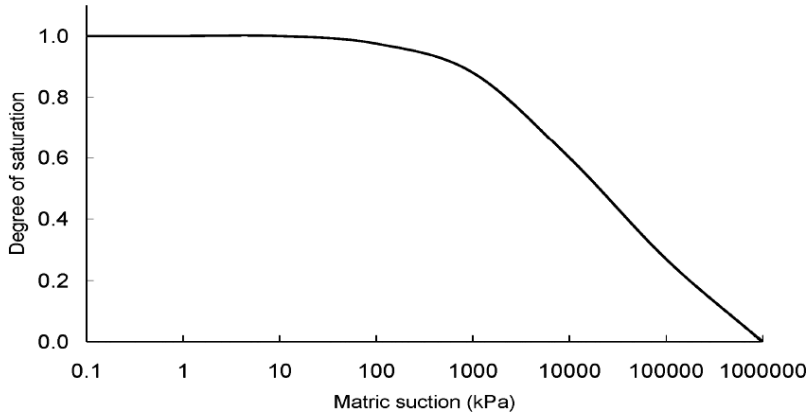

Fig. 16. Water retention curve used for this simulation[32] (reproduced after Indraratna *et al.*[30]).

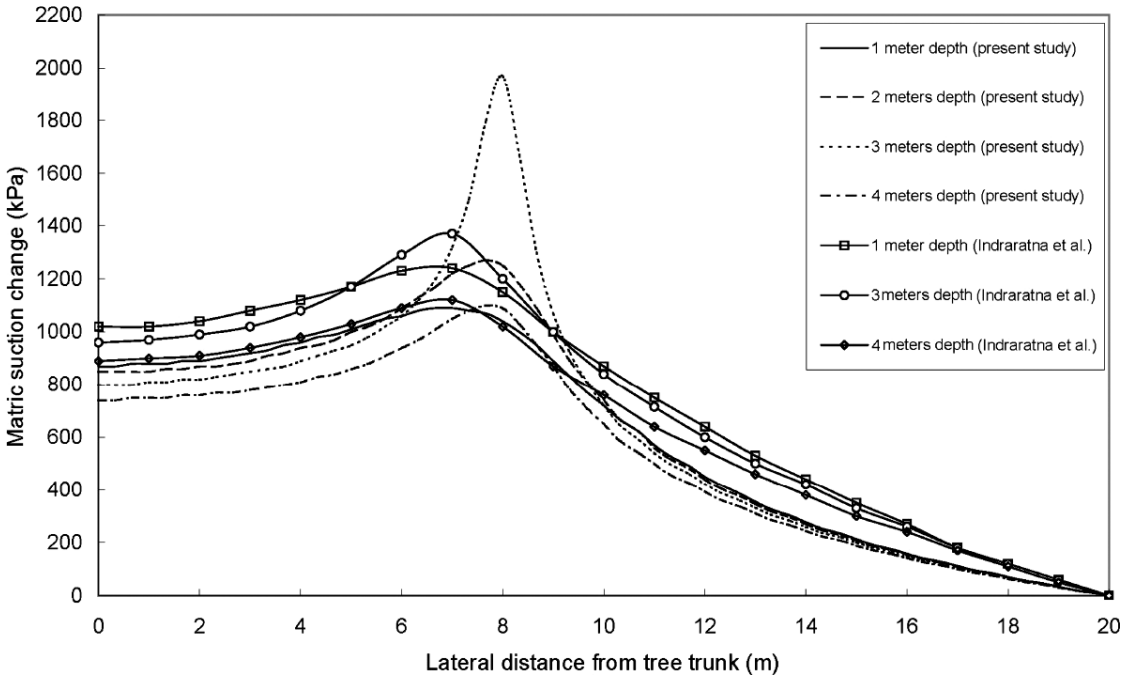

Fig. 17. Comparison of matric suction change results of present study[32] and the results of simulation done by Indraratna *et al.*[30]

where $k_s = 5 \times 10^{-9}$ m/s. Also, as suggested by Indraratna *et al.*[39] the void ratio is assumed to be unity, and the Poisson's ratio of 0.3 is applied in the simulation. The state surfaces of void ratio and degree of saturation are calibrated based on the available known parameters for the stress range of the problem.

It is observed in the numerical simulation that after one year of root water uptake, the matric suction value in different points of the soil near the tree reaches equilibrium condition and the changes become negligible during time. Hence, the matric suction results of one-year period simulation could be a good estimation of the reality. Matric suction change results obtained from the authors' model is presented in Fig. 17 in comparison with the results of the same simulation done by Indraratna *et al.*[39] Also, Fig. 18 depicts the measured total suction around the tree, reported by Jaksa *et al.*[49] Note that Fig. 18 is produced by Indraratna *et al.* doing interpolation between four measured values for each depth interval. It should be pointed out that both in this study and in the study by Indraratna *et al.*, it has been assumed that the volume of moisture evaporated from the soil surface equals the volume of water inflow. Moreover, in both studies, temperature variation during time is neglected. These assumptions are made because of the lack of field measurements.

It can be seen that numerical simulation procedure, proposed by the authors, has been successful in estimating the trend of suction production around the tree. The maximum change in suction has occurred at 3 m depth and in lateral distance of 8 m from the tree axis, which is within the range determined by Jaksa *et al.*; this is what was expected from the simulation, and is confirmed by the measurements.

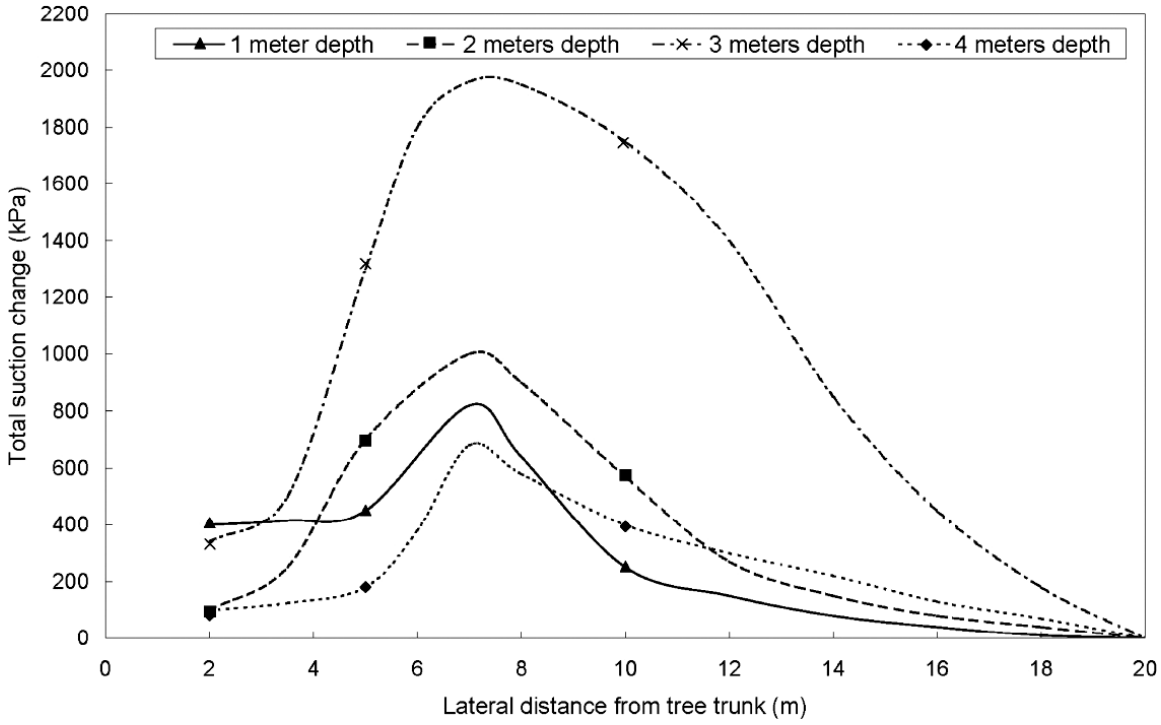

Fig. 18. Total suction change measurements[32] (reproduced after Jaksa *et al.*[30]).

The trend shows that the matric suction changes most significantly at (r_0, z_0), where we have maximum root water uptake, and the change reduces as it nears the tree axis. Also, at a lateral distance of 20 m from the tree trunk the matric suction has not experienced any changes both in the simulation and in the measurements.

Although it seems that the formulation presented in this paper has been more robust than that of Indraratna *et al.*[39] in modeling the trend and magnitude of suction change around the tree, there are some discrepancies between the simulation and the measurements. First, in the measurements, the suction change is much lower near the tree trunk than it is in the simulation. The probable reason for this difference is proposed by Indraratna *et al.* as the suction-reducing effect of irrigation near the tree trunk which is neglected in this study. The second disparity is that the real change of suction at lower depths is less than what is estimated by the authors' model. Soil heterogeneity would be the first reason. Moreover, we have neglected the effects of irrigation and water rainfall on reducing the matric suction. And finally, most importantly, it should be noted that water retention curve and unsaturated soil permeability relationships proposed by Indraratna *et al.*[39] are just approximations for typical clay soils and are not measurement based.

6. Thermohydrochemomechanical Coupling

In this part an extension of the above-mentioned model is presented in order to include the chemical effects and their interactions with the other phases. In this

extension the advection, dispersion, diffusion of contaminant, and some basic chemical interactions between the liquid phases and soil are considered. The governing equations in terms of soil displacements, water and air pressure, temperature, and nonreactive water solute concentration of contaminant are written. The final nonlinear partial differential equations are solved by finite element method. A set of equations of this part are integrated in θ-Stock by Ghasemzadeh and Gatmiri.[50]

6.1. *Field equations*

Equilibrium equation and constitutive law can be written as mentioned before. With a new term related to the rate of concentration of pollutant ($L_C dC$):

$$d(\sigma_{ij} - \delta_{ij} p_g) = D d\varepsilon - F d(p_g - p_w) - C_T dT - L_C dC\,, \tag{132}$$

$$L_C = D D_c^{-1} \quad \text{with } D_c^{-1} = \beta_c m \quad \text{in which} \quad \beta_c = \frac{1}{1+e}\frac{\partial e}{\partial (C)}\,,$$

where σ is stress tensor, p_g is pressure of gas; p_w is pressure of water, and the other terms are defined in Eq. (36). In this modeling, the state surface concept already used in THM modeling has been extended to include chemical solute concentration coupling effects with the other variables. The state surfaces of void ratio (e) and degree of saturation (S_r) are therefore of the form

$$\begin{aligned} e &= \frac{1+e_0}{\exp[\,[A]^{1-m}/K_b(1-m)]\exp(c_e(T-T_0))} - 1\,, \\ A &= a_e\left(\frac{\sigma - p_g}{p_{\text{atm}}}\right) + b_e\left(1 - \frac{\sigma - p_g}{\sigma_c}\right)\left(\frac{p_g - p_w}{p_{\text{atm}}} + \xi\frac{P_{os}}{P_{\text{atm}}}\right), \end{aligned} \tag{133}$$

$$\begin{aligned} S_r = 1 - [a_s + b_s(\sigma - p_g)][1 - \exp(c_s(p_g - p_w))] \\ \times \exp(f_s(C - C_0))\exp(d_s(T - T_0))\,, \end{aligned} \tag{134}$$

σ_c is preconsolidation stress, K_b, m, a_e, b_e, c_e, ζ, a_s, b_s, c_s, d_s, f_s and d_s are the parameters of void ratio and degree of saturation state surfaces.

Chemical species transport and their interactions with the other phases can be expressed in mass conservation equation as

$$\frac{\partial(\theta C)}{\partial t} = \frac{\partial}{\partial x_i}\left(D\frac{\partial(\theta C)}{\partial x_j}\right) - \frac{\partial}{\partial x_i}(v_i \theta C) + q_r C_r + \sum R_n\,, \tag{135}$$

$$\sum R_n = -\rho_b \frac{\partial C_s}{\partial t} - K_1 \theta C - K_2 \rho_b C_s\,, \tag{136}$$

where C is the concentration of contaminant; C_s is the concentration of contaminant in solid phase; v_i is water velocity in direction i; q_r and C_r are discharge and concentration of source; D is dispersion coefficient; Δ_b is bulk density of soil; and K_1 and K_2 are decay coefficients of solved and adsorbed concentration. Different geochemical models are used to express the relation between C_s and C as linear sorption, Freundlich sorption, Langmuir sorption, and Lungmuir two-surface

Table 2. Necessary parameters relevant to Arands *et al.* (1997) experiment.[39]

Parameter	Value
Temperature (°C)	21
Diffusion of toluene (m^2/s)	4.2e−6
Water content (w%)	6.7
Relative density (G_s)	2.52
Porosity (n)	0.5

sorption. Dispersion coefficient (D) is a function of molecular diffusion (D_m) and hydromechanic dispersion:

$$D = D_m + a(\theta)v\,, \tag{137}$$

where v is mean velocity of water.

6.2. *Physical modeling by Arands et al. (1997)*

Arands *et al.* (1997) investigated the transport of two pollutants named toluene and nitrobenzene through the unsaturated soil. In this paper, toluene transport is chosen to be numerically analyzed using the θ-Stock software.

To establish the experiments, an apparatus was built by Arands *et al.* (1997).

A cylindrical soil sample with a height of 16 cm and diameter of 7.5 cm was remolded and placed inside the apparatus chamber. Then, adequate amount of toluene solvent was provided inside the reservoir of apparatus. Solvent vapor along with air was blown through the unsaturated porous soil and the solvent was splashed over sample surface with a specific rate. Consequently, the solvent flow through unsaturated soil was established in both liquid and vapor phase.

Some necessary parameters relevant to soil sample and experimental medium in Arands tests are provided below.

6.3. *One-dimensional modeling of pollutant transport through unsaturated porous medium*

A one-dimensional numerical model is developed and analyzed using data mentioned in Table 2. The geometry of model has been shown in Fig. 19. Displacement of nodes in x- and y-directions and temperature for all nodes are restricted in this model.

The upper and the lower sides of the model are isolated from water flow. A pollutant concentration of 5.4 mol/m^3 has been injected to the model from the right side.

State surfaces for void ratio and degree of saturation are introduced to a software based on physical conditions of experiment.

The results of both Arands' experiment and numerical analysis of θ-Stock code are presented in Fig. 20 through the concentration–time graph.

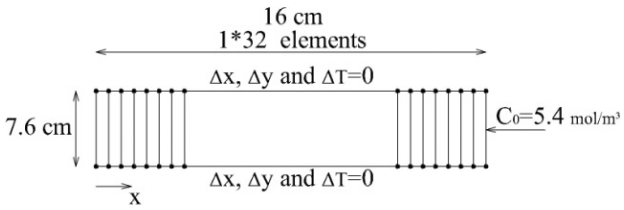

Fig. 19. Geometry of the problem.

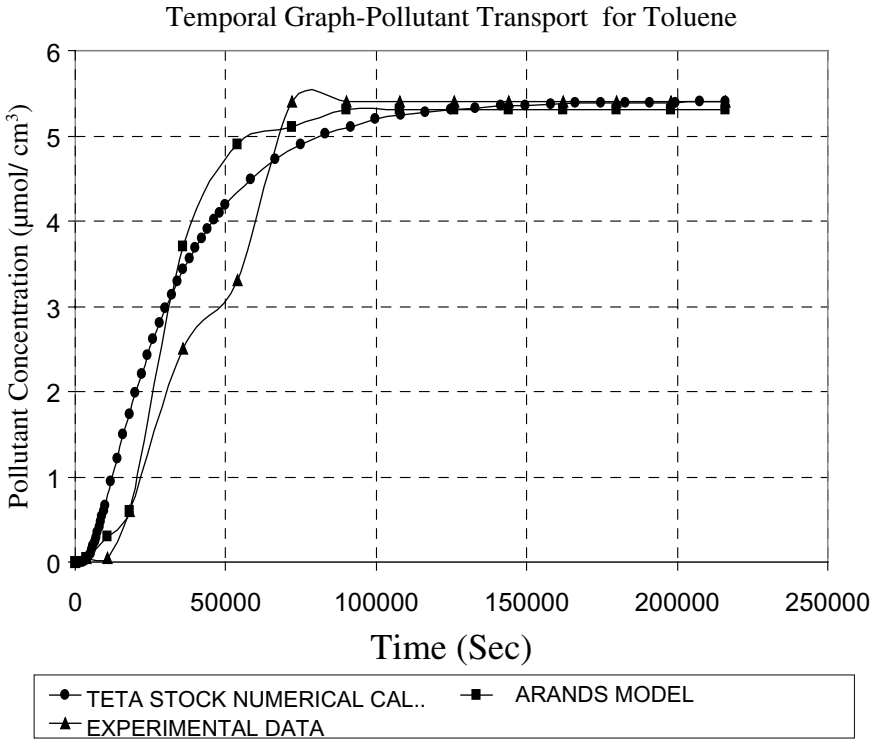

Fig. 20. Concentration–time graph — Model based on Arands *et al.* (data from Ref. 39).

7. Conclusion

The software for the finite element analysis of multiphase porous media was presented and discussed.

The exchange of moisture and heat between a multiphase soil and an atmosphere layer is simulated. The latent and sensible heat transport equations and consequently the moisture equations are considered. The climatic measured factors such as wind, temperature, precipitation, humidity, and radiation are taken into account.

A set of equations have been integrated in finite element code of θ-Stock in order to carry out a fully coupled simulation of the effect of vegetation water uptake in unsaturated porous media. The results of the simulations showed that trees have the potential to severely change the soil moisture and matric suction; this change is at a lateral distance from tree trunk. Also, they can make settlement in their vicinity

which would have destructive effects on their nearby structures especially during drought periods that atmospheric precipitation does not suffice the vegetation water demand.

A mixed damage model based on the use of independent state variables (net stress, suction, and thermal stress), combining phenomenological and micromechanical concepts is presented. Giving a description of the thermohydromechanical phenomena occurring in the EDZ in a rigorous thermodynamic and mathematical frame is a challenge which is formulated in θ-Stock.

In this paper after a brief description of governing equations of THCM behavior of multiphase porous media, the transfer of chemical solute concentration in an unsaturated deformable medium was studied by using the θ-Stock finite element code.

In each part the results of numerical modeling are compared with the available experimental test results in order to validate the model.

References

1. B. Gatmiri and P. Delage, Nouvelle formulation de la surface d'état en indice des vides pour un modèle non linéaire élastique des sols non saturés — Code U-Dam, *Proc. Unsat. Soils*, eds. E. E. Alonso and P. Delage (1995), pp. 1049–1056.
2. B. Gatmiri and P. Delage, A formulation of fully coupled thermal-hydraulic-mechanical behavior of saturated porous media — Numerical approach, *Int. J. Numer. Anal. Meth. Geomech.* **21** (1997) 199–225.
3. B. Gatmiri, Analysis of fully coupled behavior of unsaturated porous media under stress, suction and temperature gradient, Final Activity Report of CERMES (1997), p. 58.
4. B. Jenab-Vossoughi, Etude numérique de la modélisation thermo-élasto-plastique des sols non saturés, Thèse de doctorat de l'Ecole Nationale des Ponts et Chaussées (2000), p. 253.
5. B. Bonin, Deep geological disposal in argillaceous formations: Studies at the Tournemire test site, *J. Contaminant Hydrol.* **35** (1998) 315–330.
6. J. B. Martino and N. A. Chandler, Excavation-induced damage studies at the Underground Research Laboratory, *Int. J. Rock Mech. Min. Sci.* **41** (2004) 1413–1426.
7. J. Mertens, W. Bastiaens and B. Dehandschutter, Characterization of induced discontinuities in the boom clay around the underground excavations (URF, Mol, Belgium), *Appl. Clay Sci.* **26** (2004) 413–428.
8. C. F. Tsang, F. Bernier and C. Davies, Geohydromechanical processes in the excavation damaged zone in crystalline rock, rock salt, and indurated and plastic clays — In the context of radioactive waste disposal, *Int. J. Rock Mech. Min. Sci.* **42** (2005) 109–125.
9. B. Gatmiri, Fully coupled thermal-hydraulic-mechanical behavior of saturated porous media (soils and fractured rocks), new formulation and numerical approach, Final Report CERMES-EDF (1995).
10. B. Gatmiri, Thermoelastoplastic behavior of saturated porous media — Numerical approach, Final Report CERMES-EDF (1996).
11. J. R. Philip and D. A. de Vries, Moisture movement in porous materials under temperature gradents, *Trans. Am. Geophys. Un.* **38** (1957) 222–232.
12. O. Krischer and H. Rohnalter, Warmelertung und Dampfdiffiusion in feuchten Gutern, *Ver. Dt. Ing. Forschungsh* **402** (1940).

13. H. L. Penman, Gas and vapor movement in soil, *J. Agric. Sci.* **30** (1940) 437–462.
14. M. Geraminegad and S. K. Saxena, A coupled thermoelastic model for saturated-unsaturated porous media, *Géotechnique* **36** (1986) 539–550.
15. S. L. Houston, W. N. Houston and N. D. Williams, Thermo-mechanical behavior of seafloor sediments, *J. Geotech. Div. ASCE* **111** (1985) 1249–1263.
16. B. Gatmiri, P. Delage and A. Nanda, Consolidation des sols non saturés: Simulation des essais au laboratoire-application aux barrages en remblai, Rapport du CERMES-ENPC (1992).
17. M. Frémond and B. Nedjar, Damage, gradient of damage and principle of virtual power, *Int. J. Solids Struct.* **33** (1996) 1083–1103.
18. Z. Hou, Mechanical and hydraulic behavior of rock salt in the excavation disturbed zone around underground facilities, *Int. J. Rock Mech. Min. Sci.* **40** (2003) 725–738.
19. C. Arson, Etude théorique et numérique de l'endommagement thermo-hydro-mécanique des milieux poreux non saturé, Ph.D. thesis, Ecole Nationale des Ponts et Chaussées, France (2009).
20. B. Gatmiri and C. Arson, *θ*-Stock, a powerful tool of thermo-hydro-mechanical behaviour and damage modelling of unsaturated porous media, *Comp. Geotech.* **35** (2008) 890–915.
21. C. Arson and B. Gatmiri, On damage modelling in unsaturated clay rocks, *Phys. Chem. Earth* **33** (2008) S407–S415.
22. C. Arson and B. Gatmiri, A mixed damage model for unsaturated porous media, *Comptes-Rendus de l'Académie des Sciences de Paris, Section Mécanique* **337** (2009) 68–74.
23. C. Arson and B. Gatmiri, Numerical study of a thermo-hydro-mechanical model for unsaturated porous media, *Ann. Solid Struct. Mech.* **1** (2010) 59–78.
24. N. R. Hansen and H. L. Schreyer, A thermodynamically consistent framework for theories of elastoplasticity coupled with damage, *Int. J. Solids Struct.* **31** (1994) 359–389.
25. J. F. Shao, H. Zhou and K. T. Chau, Coupling between anisotropic damage and permeability variation in brittle rocks, *J. Numer. Anal. Meth. Geomech.* **29** (2005) 1231–1247.
26. Z. P. Bazant, Why continuum damage is nonlocal: Micromechanics arguments, *J. Eng. Mech. ASCE* **117** (1991) 1070–1087.
27. M. Th. van Genuchten, A closed-form equation for predicting the hydraulic conductivity of unsaturated soils, *Soil Sci. Soc. Am. J.* **44** (1980) 892–898.
28. T. H. Yang, J. Liu, W. C. Zhu, D. Elsworth, L. G. Tham and C. A. Tang, A coupled flow-stress-damage model for groundwater outbursts from an underlying aquifer into mining excavations, *Int. J. Rock Mech. Min. Sci.* **44** (2007) 87–97.
29. Z. H. Lu, Z. H. Chen, X. W. Fang, J. F. Guo and H. Q. Zhou, Structural damage model of unsaturated expansive soil and its application in multi-field couple analysis on expansive soil slope, *Appl. Math. Mech.* (*English edition*) **27** (2006) 891–900.
30. J. F. Shao, N. Ata and O. Ozanam, Study of desaturation and resaturation in brittle rock with anisotropic damage, *Eng. Geol.* **81** (2005) 341–352.
31. D. Halm and A. Dragon, An anisotropic model of damage and frictional sliding for brittle materials, *Eur. J. Mech. A/Solids* **17** (1998) 439–460.
32. X. Pintado, A. Ledesma and A. Lloret, Back analysis of thermo-hydraulic bentonite properties from laboratory tests, *Eng. Geol.* **64** (2002) 91–115.
33. S. Hemmati, Etude de l'interaction sol-végétation-atmosphère avec une approche couplée Thermo-Hydro-Mécanique, PhD. thesis, Ecole des ponts ParisTech (2009).

34. S. Hemmati, B. Gatmiri and B. Azari, Numerical modeling of the soil moisture changes due to soil–atmosphere interaction, *Proc. First European Conf. Unsaturated Soils, E-UNSAT 2008*, Durham, United Kingdom, 2–4 July 2008, pp. 791–796.
35. S. Hemmati, B. Gatmiri, Y. J. Cui and M. Vincent, Prediction of clayey soils settlements resulted by soil–atmosphere interactions and climatic conditions, *Proc. Fourth Biot Conf. Poromechanics*, Columbia University, New York, USA, 8–10 June 2009, pp. 234–239.
36. H. L. Penman, Natural evapotranspiration from open-water, bare soil and grass, *Proc. Roy. Soc. Acad.* **193** (1948) 120–145.
37. ASCE, Evapotranspiration and irrigation water requirements, *ASCE Manuals and Reports on Engineering Practice No. 70* (American Society of Civil Engineering, New York, 1990).
38. J. M. Fleureau, Z. Guellati, D. Nguyen and H. Souli, Synthèse des essais réalisés au LMSSMat sur le matériau du site de Mormoiron, Annexe de rapport BRGM, Projet ANR-05-PRGCU-005, Rapport semestriel d'activité n°3 (2007).
39. B. Indraratna, B. Fatahi and H. Khabbaz, Numerical analysis of matric suction effects of tree roots, *Proc. Institution of Civil Engineers*, Geotechnical Engineering (2006), pp. 77–90.
40. W. R. Gardner, Relation of root distribution to water uptake and availability, *Agronomy J.* **56** (1964) 41–45.
41. B. Gatmiri and M. Najari, Modeling of settlement and induced matric suction in multiphase porous media under root water uptake effect by F.E.M, *Commun. Numer. Meth. Eng.* **26** (2010) 1764–1780.
42. M. Najari and B. Gatmiri, The influence of vegetation water uptake on moisture and matric suction changes in multiphase porous media, *Fourth Biot Conf. Poromechanics*, Columbia (2009).
43. S. Hemmati and B. Gatmiri, Numerical modelling of tree root-water-uptake in a multiphase medium, *Proc. First European Conf. Unsaturated Soils, E-UNSAT*, Durham, UK (2008), pp. 785–790.
44. S. Hemmati, B. Gatmiri, Y. J. Cui and M. Vincent, Validation of a tree roots water uptake model in a finite element code θ-Stock, *17th Int. Conf. Soil Mechanics and Geotechnical Engineering*, Alexandria, Egypt (2009), pp. 843–846.
45. R. A. Feddes, P. J. Kowalik and H. Zaradny (eds.), Water uptake by plant roots, *Simulation of Field Water Use and Crop Yield* (John Wiley and Sons, Inc., New York, 1978), pp. 16–30.
46. R. Prasad, A linear root water uptake model, *J. Hydro.* **99** (1988) 297–306.
47. R. A. Feddes, P. J. Kowalik, S. P. Neuman and E. Bresler, Finite difference and finite element simulation of field water uptake by plants, *Hydrol. Sci. Bull.* **XXI** (1976) 81–98.
48. D. G. Fredlund and V. Q. Hung, Prediction of volume change in an expansive soil as a result of vegetation and environmental changes, *Proc. Conf. Expansive Clay Soils and Vegetative Influence on Shallow Foundations* (2001), pp. 24–43, doi 10.1061/40592(270)2.
49. M. B. Jaksa, W. S. Kaggwa, J. A. Woodburn and R. Sinclair, Influence of large gum trees on the soil suction profile in expansive soils, *Aus. Geomech.* **37** (2002) 23–33.
50. B. Gatmiri and H. Ghasemzadeh, Thermo-hydro-chemo-mechanical coupling in environmental geomechanics, *Fourth Int. Conf. Unsaturated Soils*, Carefree (2006).
51. B. Gatmiri and A. Hour, Excavation effect on the thermo-hydro-mechanical behaviour of a geological barrier, *Phys. Chem. Earth* **32** (2007) 947–956.